UNIVERSITAT POLITÈCNICA DE VALÈNCIA

ESCUELA TÉCNICA SUPERIOR INGENIERÍA INDUSTRIAL VALENCIA

INDUSTRIAL ENGINEERING MASTER THESIS

VELOCITY AND DROPLET SIZE OPTIMIZATION ON A DENSE DIESEL SPRAY WITH NEW PDPA EQUIPMENT

AUTHOR: Lars Degroote

SUPERVISOR: Raul Payri

Academic year: 2021-22

UNIVERSITAT POLITÈCNICA DE VALÈNCIA

ESCUELA TÉCNICA SUPERIOR INGENIERÍA INDUSTRIAL VALENCIA

TRABAJO FIN DE MASTER EN INGENIERÍA INDUSTRIAL

OPTIMIZACION DE LA MEDICION DE LA VELOCIDAD Y EL TAMAÑO DE LAS GOTAS EN UN CHORRO DIESEL DENSA CON EL NUEVO EQUIPO PDPA

AUTOR: Lars Degroote

TUTOR: Raul Payri

Curso Académico: 2021-22

ABSTRACT

For meeting the strict environmental requirements for diesel engines currently and in the near future, scientists and engineers pursue the reduction of pollutants and emissions while maintaining engine performance by cleaner combustions, analysing different fuels and injection strategies. To achieve this, the diesel spray has to be characterised for operating conditions similar to those of an actual engine. Modern diesel common rail systems operate under a very high pressure and consequently a very dense spray. In a real engine the diesel spray cannot be clearly seen and characterised, therefore, for research purposes the injector is mounted in a pressurised vessel with optical accesses for employing optical techniques diagnosis. The Phase Doppler Particle Analysis (PDPA, also known as PDA) technique is to be used to measure simultaneously droplets diameter and velocity in various locations along the spray axis. The focus of this project is optimizing the different parameters of the new PDA equipment to measure droplet velocity and the fuel pressure effect. The rough data gathered is processed by means of MATLAB to have accurate plots that represent the spray. These measurements help to understand how particulate flows move and are a solid database for the validation in CFD models.

Keywords: Diesel spray, droplet size, droplet velocity, PDPA, optical measurement

RESUMEN

Para cumplir con las estrictas restricciones medioambientales a los motores Diesel en la actualidad y en un futuro próximo, los científicos e ingenieros persiguen la reducción de los contaminantes y las emisiones manteniendo el rendimiento del motor mediante combustiones más limpias, analizando diferentes combustibles y estrategias de inyección. Para lograrlo, es necesario caracterizar el espray diésel en condiciones de funcionamiento similares a las de un motor real. Los modernos sistemas diésel common rail funcionan con una presión muy alta y, en consecuencia, con una pulverización muy densa. En un motor real, la pulverización de gasóleo no se puede ver y caracterizar claramente, por lo que, con fines de investigación, el inyector se monta en un recipiente presurizado con accesos ópticos para emplear técnicas ópticas de diagnóstico. En el presente trabajo, la técnica óptica que se utilizará es un nuevo Análisis de Partículas por Doppler de Fase (PDPA, también conocido como PDA). Esta técnica basada en la teoría Doppler es altamente especializada para medir simultáneamente el diámetro y la velocidad, siendo necesaria la utilización de un sistema de traversa para posicionarse en varias localizaciones a lo largo del eje del espray. El objetivo de este proyecto es optimizar los diferentes parámetros del nuevo equipo PDA para medir la velocidad de las gotas y el efecto de la presión del combustible. Los datos aproximados recogidos se procesan mediante MATLAB para obtener gráficos precisos que representen la pulverización. Estas mediciones ayudan a comprender cómo se mueven los flujos de partículas y constituyen una sólida base de datos para la validación en modelos CFD.

Palabras clave: Chorro de diésel, diámetro de gotas, velocidad de gotas, PDA, técnicas ópticas.

TABLE OF CONTENT

FIGURE LIST

TABLE LIST

CHAPTER 1. PROJECT APPROACH

1. 1. Company Presentation and Teamwork

The project was carried out at the Instituto Universitario De Motores Térmicos - CMT of the University “Universidad Politécnica de Valencia”. Its realization was under the direction of Dr Raul Payri, direct responsible for the project and PhD student Victor Mendoza.

1. 2. Motivation

The PDA measurement technique allows to know the size and velocity of particles in a stream, such as droplets in an injection spray. It is an extension of LDA (Laser Doppler Anemometry) which was developed by Yeh and Cummins in 1964 [1] and has since undergone rapid development, becoming very important for the study of diesel injection nozzles in the 1990s. The need for constant improvement in order to comply with European regulations on smoke and polluting emissions (Euro VI) has put the study of diesel jets with PDA back in the spotlight, since it makes it possible to know the diameter and velocity distribution of the droplets, which can be compared with the results obtained from CFD simulations in order to validate their accuracy. The aim of this work is to produce a document that presents all the parameters and procedures to be taken into account when setting up this measurement system and which, although they do not usually appear in manuals or descriptions of the experimental set-ups used, are fundamental for the correct use of the PDA technique.

1. 3. Objective

The objective in this work can be divided into 3 main ideas. The first part is setting up the PDA and other operating devices to establish the best configuration to further on execute PDA measurements. This part also includes the finding of the spray orientation and the orientation of the probe volume, once these are known, the reference from one to another must be acquainted. The second part is actually measuring the droplet velocities. A step by step process to obtain data is given at section 4. 5. Acquire PDA data. The third part is plotting the obtained data to optimize the configurations set to execute PDPA measurements. These measurements provide the necessary information to display a graphical representation that will help us to understand how the input variables effect the behaviour of the spray during the injection process.

To have a clear characterization of the spray, measurement data needs to be acquired in different positions within the spray and along the spray axis. Then it is possible to compare data at Z location 50, 70, and 90 millimetre distant from the orifice, along the spray axis to witness

similarities and differences. Measurements in one fixed Z position are varying in X and Y, there are 3 patterns that can be followed, the first one is both Z and Y are fixed and the measurement volume moves just in X through the middle of the spray, then the same can be done but now Z and X are fixed so the measurement volume moves in Y through the middle of the spray.

1. 4. Determining the purpose

When designing new technologies, achieving high efficiency is of fundamental importance when it comes to conserving energy resources, since it is a requirement of the law and, above all, an attitude of human consciousness that wants to contribute to sustainable development. In new concepts of power generation with internal combustion engines, the injection system plays an important role when it comes to achieving high efficiency. Therefore, optimizing the measurement system helps towards a better understanding how the injection system effects a clean combustion.

CHAPTER 2. INTRODUCTION

2. 1. General context

2. 1. 1. History

A diesel engine is a piston engine that works on the principle of self-ignition, when air is compressed the temperature of the air rises where at high compression the temperature is high enough to make the fuel injected under high pressure spontaneously combust. [2] The history of the diesel engine begins in 1892, Rudolf Diesel is the inventor and namesake of the diesel engine. At that time he applied for a patent for a new and economical combustion engine and he convinced, amongst others, the management of the Maschinenfabrik Augsburg to invest into the development of his engine. At the beginning of 1897 the prototype seen in Figure 1 ran satisfactorily and two more models were produced. In 1913 Rudolf Diesel died, his financier the managing director of the Maschinenfabrik Augsburg- Nuremberg (later the MAN truck manufacturer) continued to develop the engine. In 1924 the first diesel truck branded MAN made its first long run test from Augsburg to Nuremberg – MAN's headquarters in Germany. The 155 km trip took five hours and the MAN engineers who drove it spoke of a smooth journey on arrival, this first diesel truck was in use for decades afterwards without any major failures.

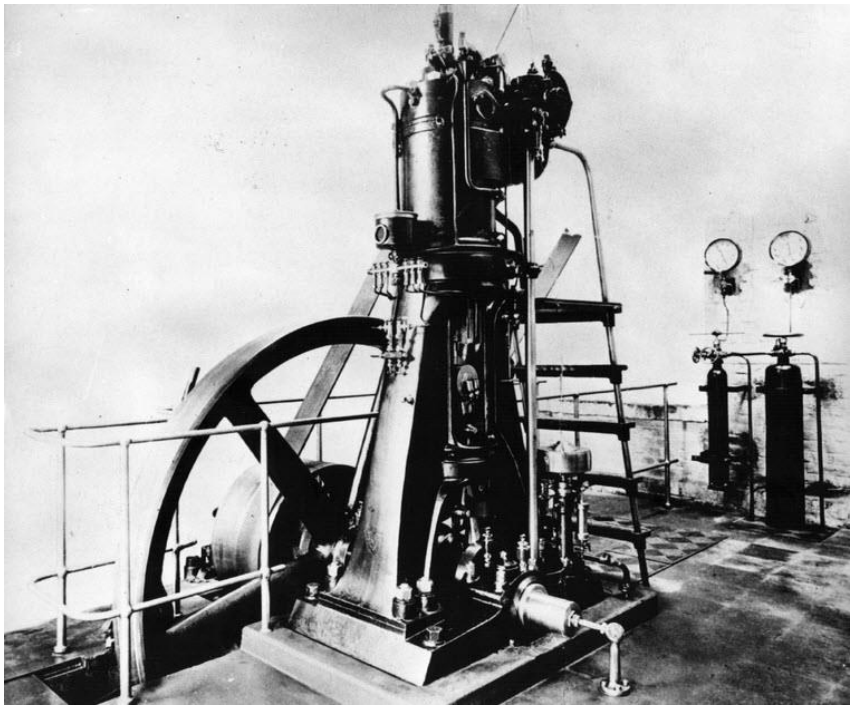

Figure 2.1. The first Diesel engine designed by Rudolf Diesel [3]

Originally diesels were only suitable for stationary use, for example in factories and mining, because they only ran at a fixed speed. Due to the high compression ratio these diesel engines caused a lot of vibration and noise, therefore the engines had to be made extra heavy. It was not until Robert Bosch developed an injection pump in the early 1920s [4] with chich the fuel supply and thus the engine speed could be regulated that the diesel engine also became interesting for the automotive industry. Manufacturers gradually developed smaller and lighter diesels that caused less vibration and noise and were suitable for use in vehicles. The first of these was the MAN truck in 1924.

In the 1930s Mercedes-Benz and Peugeot brought diesel variants of their commercial vehicles onto the market. Peugeot was also working on a diesel passenger car, but the Second World War threw a spanner in the works. The first diesel passenger car was the Hanomag Rekord in 1933, followed by the Mercedes 260D in 1936 [5]. Mercedes-Benz and Peugeot were the only ones to offer diesel passenger cars until Fiat introduced a diesel version of the 1400 in 1953 almost 20 years later. Both Mercedes and Peugeot were often used as taxis, known to be slow and emitted a lot of soot. The breakthrough of the diesel engine on the private market came at the end of 1979 with the introduction of the Volkswagen Golf Diesel.

Compared to petrol engines, diesels were always significantly slower and delivered less power but thanks to the use of a turbocharger, the turbo-diesel engines is on a par with its petrol equivalent. The turbo not only provides more specific power, but also more efficiency, lower emissions and less noise. In Europe, the Peugeot 604 was the first passenger car with a turbo-diesel engine in 1979. Mercedes-Benz was ahead of Peugeot with the 300SD, but this was only sold in the United States and Canada from 1977.

In the 1980s it was considered environmentally friendly to drive on diesel fuel although the newly legalised Liquefied Petroleum Gas (LPG) was even greener. Although the installation and risk of explosion LPG had, kept many people away. The average car driver of the time assumed that because a diesel car consumed less, it also polluted less and was therefore more virtuous. Moreover in those days lead was used in petrol to improve the octane number, lead was an evil that had to be combated so it got replaced by benzene which was later discovered to be carcinogenic. Moreover petrol engines at the time often still used a carburettor which has a low efficiency compared to the diesel engine with its high volumetric ratio and injectors. The Fiat Croma innovated in 1988 with the 1.9 TDiD with Bosch direct injection together with the Austin Montego it marked the beginning of a new trend.

2. 1. 2. Diesel applications

The diesel engine is used worldwide in large numbers, especially in the transport industry but also for stationary purposes. Over the years the diesel engine has developed further and further and due to the series production, the costs are lower than other emerging technologies such as Organic Rankine cycle (ORC) and Stirling engines. Another advantage is a large possible range of power capacities where at all ranges it is adjustable power that is more robust than gas engines and slightly higher efficiency due to the higher compression ratio. Diesel engines provide both mobile and stationary usage and are ideal for self-propelled applications where a fast change of power is required.

2. 1. 3. Diesel emissions

Diesel engines have a number of disadvantages that are similar to internal combustion engines, such as maintenance, emissions and noise. An important difference is the higher emission of soot particles and nitrogen oxides NOx, which are detrimental to public health. Compared to a Petrol engine, a diesel engine has more harmful emissions of NOx and Sulphur Oxide Sox therefore, DPF Diesel Particulate Filter DPF or Soot filter is added. Soot filters trap soot particles from the exhaust and retain the solid particles until the particles are oxidized or burned at high temperature inside the DPF. Biodiesel does not contain any sulphur and so the formation of SOx will not occur in comparison to fossil diesel. The efficiency of a diesel engine is higher than that of a petrol engine, therefore fuel consumption is lower for the same performance, and so are carbon dioxide emissions [6]. As an example comparing the same car model but with gasoline or diesel engine, diesel cars confirmed an advantage of ca. 20% higher fuel efficiency but, the average NOx emission factor is about three times higher than their gasoline equivalent. It is expected that the combination of biodiesel and high efficiency combustion will give the diesel engine an important place in reducing environmental concerns of the transportation sector in the future.

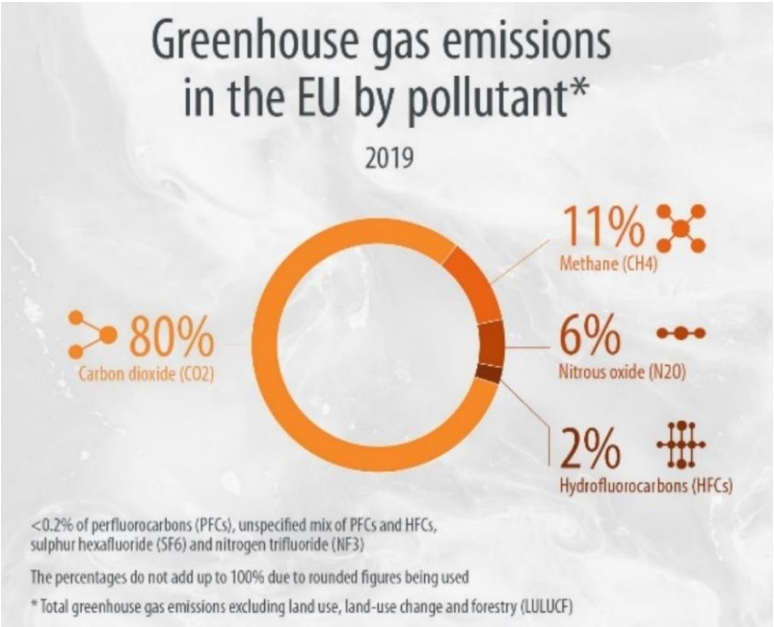

Figure 2.2. Greenhouse gas emissions in the EU by pollutant [7]

Humans are the main cause of global warming. Since the industrial revolution, we have been emitting more and more greenhouse gases. We use fossil fuels in factories, power stations, to heat our homes and for transportation. The best known emission that is mostly talked about is CO2. As the infographic Figure 1.2 shows, CO2 is the largest greenhouse gas emitted in quantity that contribute to causing climate change. Mostly it is produced by human activities. [8]

Transport is responsible for more than 30% of the EU's total transport sector CO2 emissions, a total of 72% of which come from road transport see Figure1.3 [9]. As part of its efforts to reduce CO2 emissions, the EU has set itself the target of reducing transport emissions by 60% by 2050 compared with 1990 levels. As the pace of emissions reduction has slowed, the goal of reducing CO2 emissions from transport will not be easy. Other sectors have reduced emissions since 1990, but as people become more mobile, CO2 emissions due to transportation is increasing. [9]

Efforts to improve the fuel efficiency of new cars are also declining, after a steady decline, newly registered cars in 2017 emitted an average of 0.4 grams of CO2 per kilometre more than the previous year. To curb the trend, the EU is introducing new CO2 emissions targets aimed at reducing harmful emissions from new cars and vans. For new trucks there is also a target that is to reduce CO2 emissions by 30% by 2030 compared to 2019.

CO2 emissions from passenger transport vary considerably depending on the type of transport. Passenger cars are a major polluter and account for 60.7% of total CO2 emissions from road transport in Europe. Modern cars could be among the cleanest means of transport, but this only applies if they carry more than one passenger. With an average of 1.7 people per car in Europe, other modes of transport such as buses are currently a cleaner alternative.

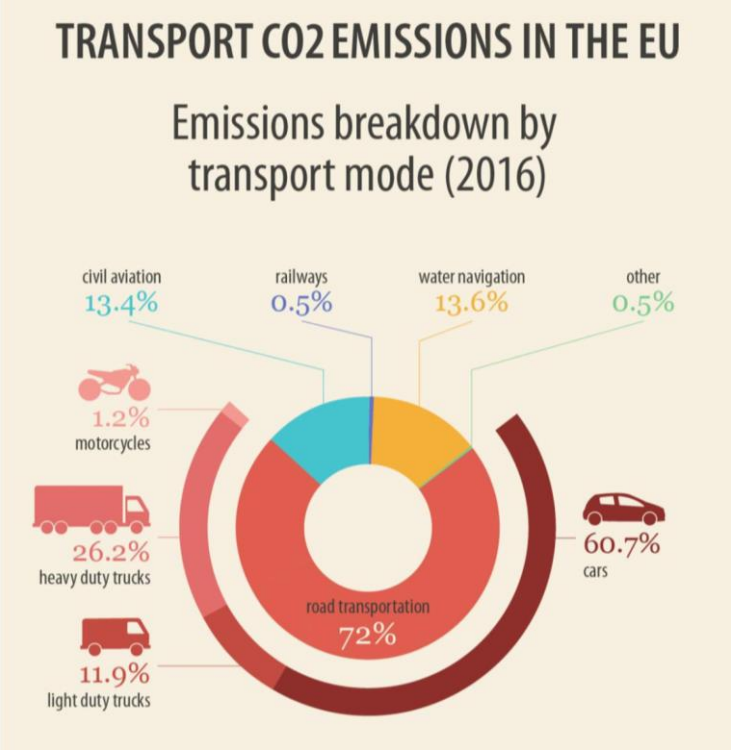

Figure 2.3. Transportation CO2 emissions in the EU [9]

2. 2. Diesel injection process

A diesel engine operates without external ignition, it sucks in air and compresses it to a much higher value than usual for an Otto engine. Due to this high compression, the final compression pressure and therefore temperature is very high, high enough to ignite the fuel that is injected into the engine at that moment. Diesel engines used to be fitted with a pre-chamber or swirl chamber, which meant there was a shared combustion chamber. Direct injection engines have a non-shared combustion chamber and therefore have higher thermal efficiency and lower fuel consumption. For this reason, Direct Injection DI engines are almost exclusively used in new vehicles today [10]. The diesel engine is ideally suited to turbocharging. Turbocharging not only increases efficiency and power output, but also reduces harmful emissions and engine noise.

The fuel is injected into the combustion chamber under high pressure, initially this jet of fuel collides with the air molecules, stripping them off and turning into a cone-shaped plume. In order to improve the distribution of fuel across the fuel chamber, multi-hole nozzles are used. When injecting with multi-hole nozzles, there is a large amount of air between the fuel plumes that cannot come into contact with the fuel droplets. Therefore, the movement of the air in the combustion chamber is very important, called swirl or turbulence. When injecting the fuel into the combustion chamber, it is impossible to give the fuel particles a path other than a straight one, which makes it difficult to bring them to the oxygen atoms. However, the air can be brought to the fuel by inducing a movement of the air drawn in. To succeed a better mixture of air and fuel, a rotating movement, a kind of swirl can be provoked via different methods like the incoming air (shape of the inlet) and compression of the air who depends on the shape of the cylinder [11]. Following points are further discussed: atomization process and combustion.

2. 2. 1. Atomisation

In order for the mixing process to be as fast as possible, the greatest possible contact between the fuel and oxygen is required. The injection spray needs to change from a dense liquid to a cloud of droplets to improve the air fuel mixture. The size of the droplets is varying but smaller droplets are preferred as these will vaporize first.

A numerical example to illustrate the importance of good atomisation goes as followed: if a fuel droplet with a diameter of 1mm is divided into 1000 droplets of 0.1mm diameter, the total area covered by these droplets will be 100 times larger than that of a single droplet of 1mm. However, the droplets must have enough mass to penetrate sufficiently far through the compressed air.

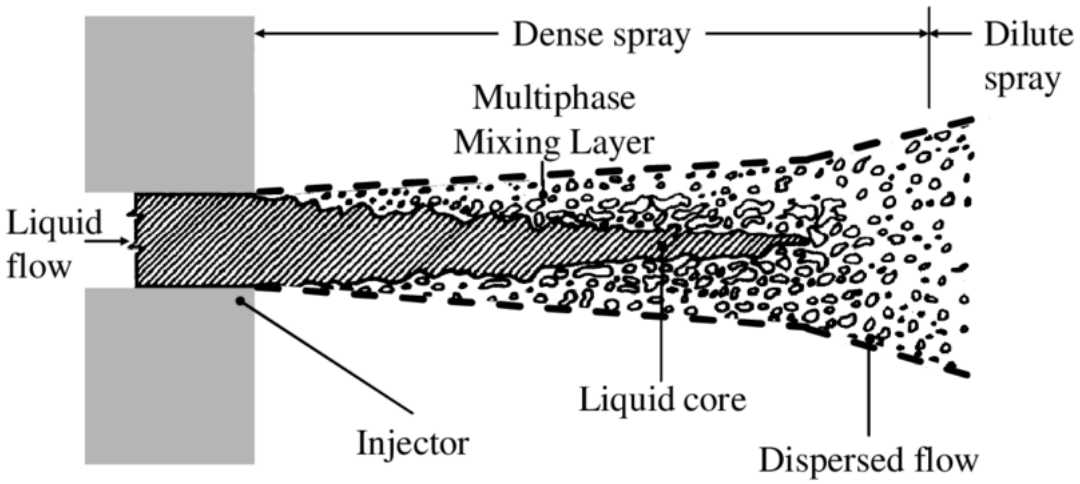

Figure 2.4 Sketch of the near-injector region of a pressure-atomised spray [12]

2. 2. 1. The combustion

The composition of the air-fuel mixture is of great importance for the fuel consumption, exhaust emission and noise of diesel engines. The influence of the injection system on the quality of the mixture is obviously very large. Ignition delay is an important factor to take into account to determine when to inject, it is the time that elapses between the injection of the fuel and its ignition. This delay is caused by both physical and chemical delay, during the physical delay, the small droplets of diesel heat up through contact with the compressed air. Before ignition takes place, the mixture of the fuel and oxygen occurs. This chemical delay lasts between 1 and 2 milliseconds [11].

The fuel injected during the ignition delay burns abruptly, causing an increase in pressure and temperature, called diesel knock. The combustion peak pressures created during the diesel knock largely determine the load on the engine's bearings. To obtain the best operating conditions, it is necessary to use fuel that ignites as quickly as possible, which implies a short ignition delay. Contrary to what is required for a petrol engine, for diesel fuel it is important to provoke a self-ignition as fast as possible. If it is delayed, too much fuel accumulates during the ignition delay and causes an explosion that is too great at the moment of ignition.

CHAPTER 3. PDA OPERATING PRINCIPALS

3. 1. Doppler theory

3. 1. 1. Introduction

The advent of the laser has made it possible to develop a completely new method of measuring velocities. In 1964, it was demonstrated for the first time that the speeds of liquids and gases can be determined using Doppler shift laser light [13]. By intersecting two narrow monochromatic light beams, a measuring volume is delimited. The particles that move through this volume reflect the laser light with a frequency that is shifted compared to the frequency of the original laser light. The scattered light thus contains the Doppler shift from which the speed can be found.

The laser doppler velocity measurement has a number of advantages over other techniques:

Advantages LDA

1. The flow is not disturbed by inserted measuring probes.
2. There is a linear relationship between frequency shift and velocity
3. A high special resolution is possible. With the laser beams a small measuring volume can be made so that the speed can be determined locally. The measurement volume is an ellipsoid with a long axis
4. The measurements are not influenced by pressure and temperature, in contrast to the pitot tube and hot wire anemometer.
5. Measurements can be made under difficult conditions where other methods cannot be used, e.g. in flames.

Disadvantages LDA

1. The measurement location must be optically accessible, so application of windows is necessary.
2. The medium must be transparent
3. There shall be a sufficient number of particles in the medium, which are small enough to follow the flow.
4. The required equipment is expensive

3. 1. 2. Doppler shift

The change in the frequency of a wave due to the relative motion of source and receiver is called the doppler shift. The name Doppler shift is also used when the frequency shift is caused by a particle reflecting the wave, this is the case with laser doppler velocity measurements. The doppler shifts are often so small that they cannot be measured directly [14].

An observer who moves away from a stationary light source at speed U will observe this light with a frequency: 2.1

$$f = f_0\left(1 - \frac{U}{c}\right) \qquad \textbf{Eq. (3.1)}$$

Where f_0 is the original frequency of the light and c is the speed of light. A stationary observer will perceive a light source that is moving towards him with a frequency:

$$f = \frac{f_0}{1 - \frac{U}{c}} \qquad \textbf{Eq. (3.2)}$$

Then consider figure 2.1 the particle P has a speed U . The particle moves through the measuring volume created by the two intersecting laser beams. Each beam has a frequency f_0.

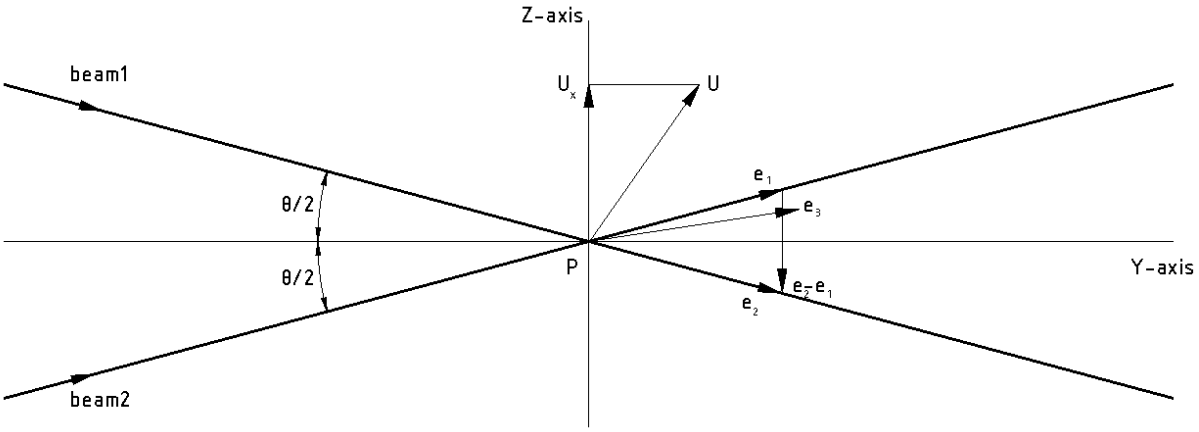

Figure 3.1. Frequency shift caused by moving particle P

P moves with a speed $\vec{U}.\overrightarrow{e_1}$ in the direction of $\overrightarrow{e_1}$ (the unit vector of beam 1) and observes the light of beam1 with a frequency:

$$f_{P1} = f_0\left(1 - \frac{\vec{U}.\overrightarrow{e_1}}{c}\right) \qquad \textbf{Eq. (3.3)}$$

The particle will scatter the light with the same frequency in all directions. The scattered light in the direction of $\overrightarrow{e_3}$ is perceived by a stationary observer at a frequency:

$$f_{ob1} = f_0\left(1 - \frac{\vec{U}.\overrightarrow{e_1}}{c}\right) = f_0\frac{\left(1 - \frac{\vec{U}.\overrightarrow{e_1}}{c}\right)}{\left(1 - \frac{\vec{U}.\overrightarrow{e_3}}{c}\right)} \qquad \textbf{Eq. (3.4)}$$

The observer sees the stray light generated by beam 2 with a frequency:

$$f_{ob1} = f_0\frac{\left(1 - \frac{\vec{U}.\overrightarrow{e_2}}{c}\right)}{\left(1 - \frac{\vec{U}.\overrightarrow{e_3}}{c}\right)} \qquad \textbf{Eq. (3.5)}$$

The stationary observer is the receptor that directs the captured stray light to a multiplier. The photomultiplier produces an electrical signal that is proportional to the intensity of the incoming light. However, the photomultiplier has a finite bandwidth and is not able to register the frequencies of vibrating light of the order $f_0 = 10^{14}Hz$. When the two light beams interfere with each other the intensity variations happen at a frequency within the bandwidth of the photomultiplier, so it is able to register this frequency. The frequency of the intensity variations is:

$$f_d = |f_{ob1} - f_{ob2}| = \frac{f_0}{c}.\left|(\vec{e}_2 - \vec{e}_1).\vec{U}\right| \qquad \textbf{Eq. (3.6)}$$

Where it is assumed that $\vec{U}.\overrightarrow{e_3} \ll c$

The photomultiplier produces an electrical signal that is proportional to f_d but independent of the sign. The direction of the velocity can therefore not be known in the way. It follows from Eq.(2.6) that f_d is proportional to the component U_x, of the velocity. The component of the velocity that is measured is the component that is perpendicular to the bisector of both laser beams (Z-axis). Using $|\vec{e}_2 - \vec{e}_1| = 2.\sin\left(\frac{\theta}{2}\right)$, Equation (2.6) can also be written as:

$$f_d = U_x\left(\frac{2.\sin\left(\frac{\theta}{2}\right)}{\lambda}\right) \qquad \textbf{Eq. (3.7)}$$

Where $\lambda\left(=\frac{f_0}{c}\right)$ is the wavelength of the incoming laser light.
f_d is the Doppler shift, who is independent of the direction $\overrightarrow{e_3}$. The sign of f_d can be determined by giving one of the beams a frequency shift f_s Suppose beam 1 has a frequency $f_0 + f_s$, then instead of formula (2.6) we have:

$$f_d = \frac{f_0}{c}(\vec{e}_2 - \vec{e}_1).\vec{U} + \overrightarrow{f_{s1}} \qquad \textbf{Eq. (3.8)}$$

Where it is assumed that $\vec{U}.\overrightarrow{e_1} \ll c$.

For a positive value of the first term, one finds a higher value for f_{ds}, and for a negative, a lower value. Now we have to choose f_s in such a way that for the greatest negative value of the first term f_{ds} is still positive.

3. 2. Dual beam method

The stray light is generated by two laser beams of equal intensity [14]. Since f_{ds} is independent of the direction of $\vec{e}_3$ (Eq. (3.8)), the stray light can be captured with a receptor. The signal is often still too weak for a photodiode, so a photomultiplier must be used. Normally, the stray light can be captured at any angle, but the following two methods can be distinguished:

3. 2. 1. Forward scatter method

The stray light is collected at the backside of the particles (at a chosen scattering angle right of the Z-axis). This method is the one used in the PDA configuration, further explanation is given at 4. 3.

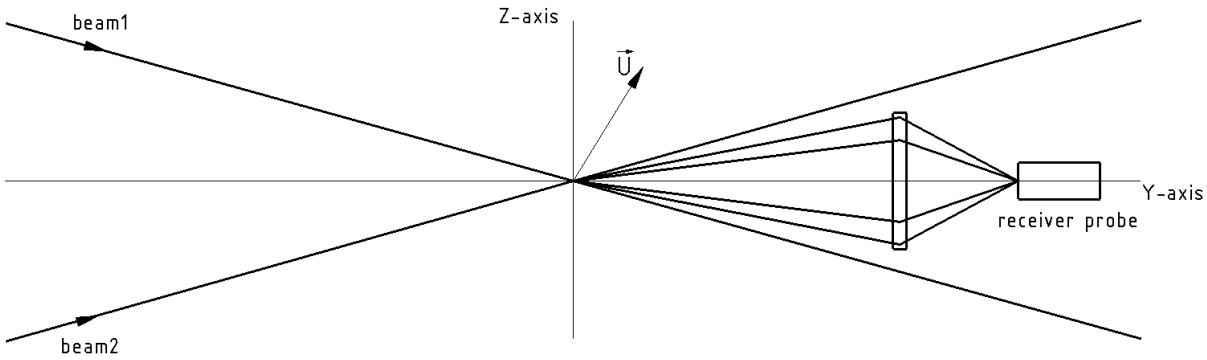

Figure 3.2. Forward scatter method

3. 2. 2. Backscatter method

The stray light is collected at the frontside of the particles (at a chosen scattering angle left of the Z-axis). The stray light can be received by the same optics as the laser beams are emitted. This simplifies the optical setup as the receiving part does not has to positioned, and the particle needs only optical access from one side. This is the method used in the LDA configuration.

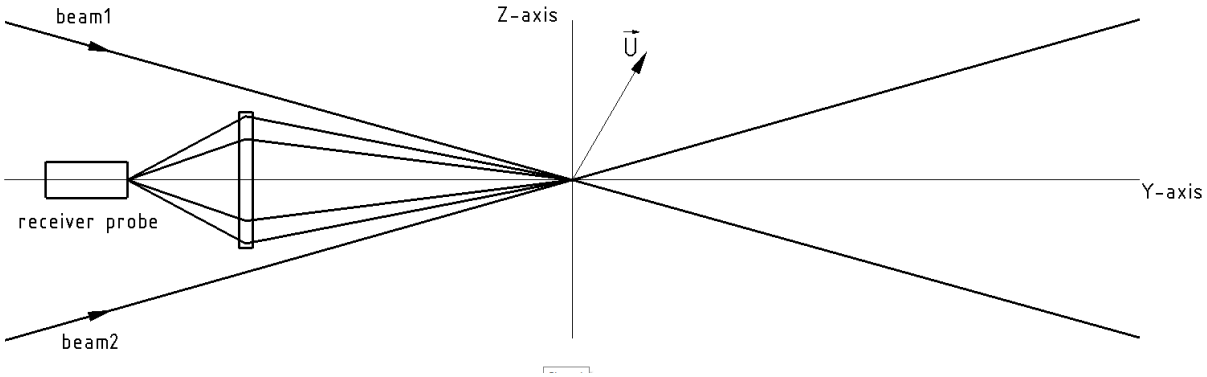

Figure 3.3. Backscatter method

3. 3. Fringe pattern to velocity

3. 3. 1. Fringe pattern

The effect of the dual beam method can also be explained without using the Doppler principle [13], [14]. Two intersecting coherent light beams produce an interference pattern in the measuring volume of alternating light and dark areas crossed by the particles. The laser beams have a Gaussian intensity distribution across the beam. The edges of the beam are those points where the intensity is reduced to $\frac{1}{e^2}$ of the maximum intensity. A laser beam is not parallel but has the course shown in Figure 3.4.

Figure 3.4. Cutting laser beams Fringe pattern [15]

The minimum diameter of the beam is called "waist". The smallest measurement volume is obtained by cutting the two laser beams at the location of the waist. In the measurement volume, a fringe pattern is created as shown in Figure 3.4. To obtain a sharp interference pattern, it is important that the beams have the same polarisation direction, that the electric field of each beam is moving in one direction e.g. vertical. The distance between the fringes can be determined with the aid of Figure 3.5 and Figure 3.6. At point P, amplification occurs when:

$$x_1 - x_2 = n.\lambda \qquad \textbf{Eq. (3.9)}$$

Where λ is the wavelength of the laser light and $n = 0, 1, 2, 3, \ldots$

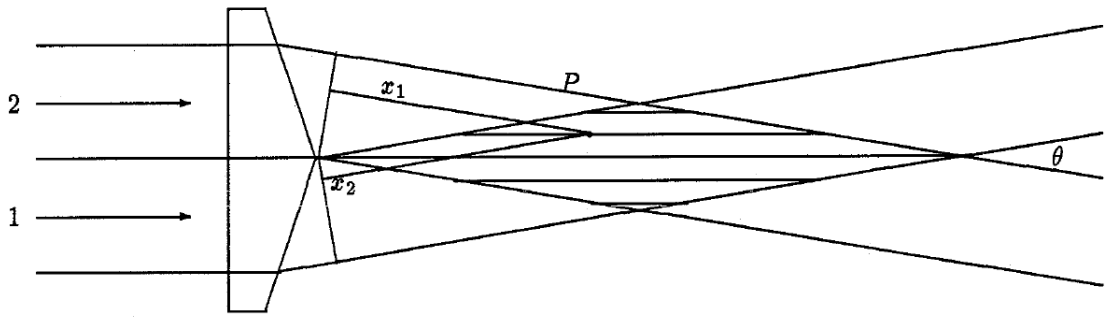

Figure 3.5. Fringe pattern of two crossing beams at angle theta [14]

Points that meet Eq. (3.9) are located on horizontal lines. The distance s between two successive

lines is shown in Figure 3.6:

$$s = \frac{\lambda}{2.\sin\left(\frac{\theta}{2}\right)} \qquad \textbf{Eq. (3.10)}$$

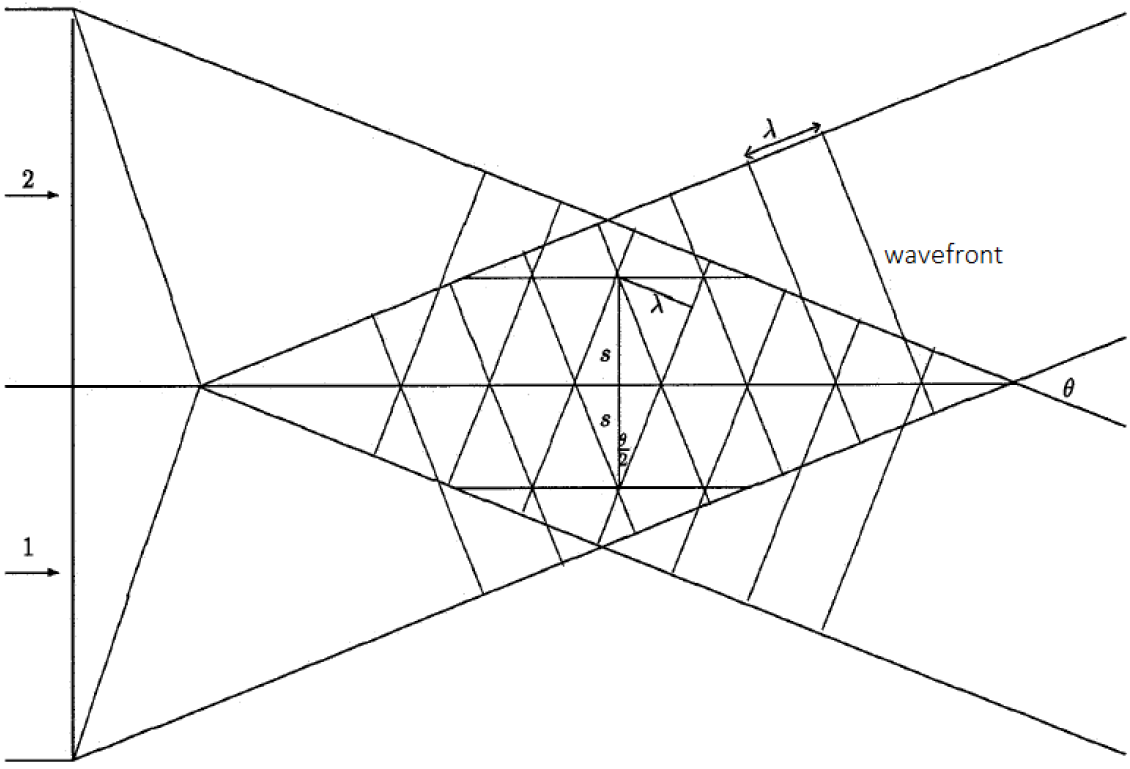

Figure 3.6. Determine fringe distance s [14]

If both beams have the same frequency f_0, the interference pattern in the measurement volume is stationary. If the frequencies of the beams are different (beam 1 : $beam1$: $f_0 + f_s$ and $beam2$: f_0), the interference pattern "rolls", with a speed:

$$u = f_s.s = \frac{f_s.\lambda}{2.\sin\left(\frac{\theta}{2}\right)} \qquad \textbf{Eq. (3.11)}$$

in the opposite direction of positive flow. The frequency shift f_s in the setup used (Dynamics FlowExplorer) is 80 MHz [16]. In order to eliminate directional ambiguity, the frequency of one of the beams is shifted by a fixed amount f_s, using a Bragg cell so that the fringe pattern “rolls” through the measuring volume with a known velocity.

3. 3. 2. Velocity

Particles crossing the measurement volume, and scatter light that is proportional to the Doppler frequency f_d [14]. A typical Doppler burst or signal from a particle is shown in Figure 3.7. If the optical system is correctly aligned, the Doppler frequency f_d for each individual fringe (s) within the measurement volume is a constant. This means that the velocity of each individual particle can be represented as

$$U = f_d . s \qquad \textbf{Eq. (3.12)}$$

U is the instantaneous velocity perpendicular to the fringes and f_d is known as the instantaneous Doppler frequency. This leads to the following equation:

$$U = f_d . s = \frac{f_d . \lambda}{2 . \sin\left(\frac{\theta}{2}\right)} \qquad \textbf{Eq. (3.13)}$$

which shows that the instantaneous particle velocity U varies linearly with f_d, since for each optical geometry and laser, $\frac{\lambda}{2.\sin\left(\frac{\theta}{2}\right)}$ is a constant. This relationship also shows that the system does not need to be calibrated [17].

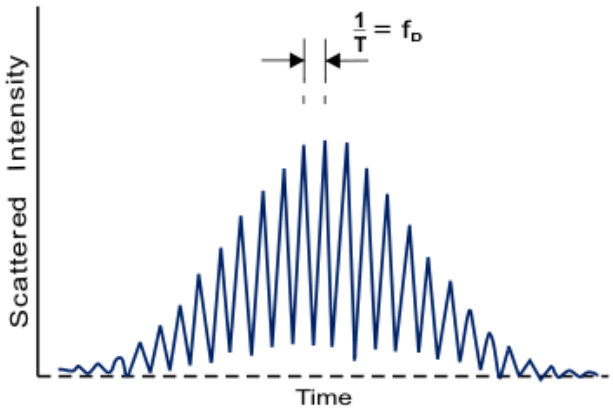

Figure 3.7. Typical Doppler burst [18]

3. 3. 3. Diameter

To be able to measure simultaneously velocity and droplet size, an extension on LDA (Laser Doppler Anemometry) was made to measure the size of spherical liquid particles called PDA Phase Doppler Anemometry. The light which is entering the droplet causes tree ways to transmit, first is reflection from the surface sphere, second is forward refraction through the droplet so the light scatters out at another angle and third is backwards refraction after an internal reflection. The intensity and the direction of the scattered light is depending on the refractive index [14].

Here the interest is on the refracted light, because the light travels through another medium, in this case a fuel droplet. The difference in the optical path causes a phase shift based on Bachalo and Houser [19]. When 2 photodetectors are receiving light they will give the same burst signal, but with this phase difference between them. The droplet size can be derived from this phase difference, but for larger droplets there can be a phase shift larger than 2π, causing an ambiguity. To eliminate this ambiguity a third photodetector is added to the system, this brings along a second phase difference but with a lower resolution to determine the size range of the droplet. Using three detectors provides both a large measurable range (ϕ_{1-3}) and a high measurement resolution (ϕ_{1-2}).

Relationship between phase shift and diameter is as followed for refraction [20]:

$$\Phi = \frac{-2\pi D}{\lambda} \frac{n_{rel} \sin\theta \sin\psi}{\sqrt{2(1+\cos\theta\cos\psi\cos\varphi)\left(1+n_{rel}^2 - n_{rel}.\sqrt{2(1+\cos\theta\cos\psi\cos\varphi)}\right)}}$$

With:

$\mathrm{n_{rel}} = \frac{\mathrm{n_{Particle}}}{\mathrm{n_{Medium}}} =$ relative refractive index

$\theta =$ depending on the beam spacing

$\varphi =$ scattering angle

$\psi =$ elevation angle

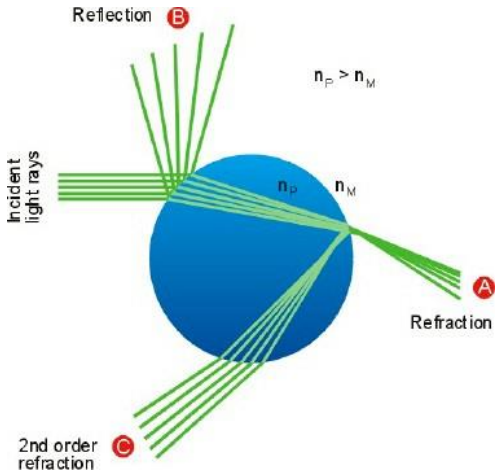

Figure 3.8. Reflection and refraction of light in a droplet [20]

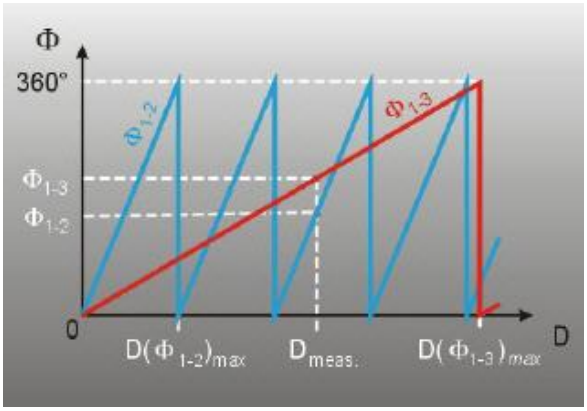

Figure 3.9. Phase difference measure by 3 photodetectors [20]

CHAPTER 4. MATERIALS AND METHODS

4. 1. Methodology

This section briefly explains the methodology and structure of the project. When a multi-hole diesel injector is analysed with a PDPA system a proper optical access in the test rig is essential. In this manner, laser beams from the PDPA system are allowed to get into the chamber and create a probe volume in the spray that will be measured. Since only one of the sprays was planned to be measured, and with the objective of that both incident and receiver beams of the PDPA can access the spray of interest.

Different injection conditions have been tested. Experiments were carried out at injection pressures 470 and 1200 bar for ambient air density 2 kg/m3. The ambient temperature was the standard of 298 K used as a reference in order to study the spray under no-evaporating conditions. For each operating point, the objective was to gather 10000 droplets to get representative data. Due to the high droplets concentration common for these sprays, measurements at axial distances below 20 mm are almost impossible [21]. Therefore, three axial locations were studied (50, 70 and 90 mm from the nozzle tip). Moving the measuring probe volume across the spray and along the radial direction diagonal in the XY plane, to limit as much as possible the passing of the beams through the spray.

Before making the whole setup, many tests were done seen in 4. 4. , each of which comes down to knowing the location of the spray in relation to the PDA equipment. Based on these tests, the orientation from the travers system or probe volume is correlated to the orientation of the spray to carry out measurements that correspond to the chosen position.

When raw data is collected with the PDA equipment it is exported to a .txt file. By means of MATLAB software graphs concerning different information are displayed in a detailed visual manner in order to draw the necessary conclusions.

4. 2. Injection system devices

4. 2. 1. Flow in system

In order to have representable data from the measurements, the conditions in the laboratory need to be similar to those of an actual engine. To obtain these similar conditions the injector is mounted in a pressurised vessel with optical accesses for employing optical techniques diagnosis. The vessel is part of a closed system with gas flowing through, the flow enters via the top part of the vessel and goes out via the bottom shown in Figure 4.1. This flow is applied to have little noise disturbing the probe volume, explanation is as followed. To obtain enough data, multiple injections are done on each position depending on how high the data rate is. Doing so accumulates a cloud of diesel particles, floating around the vessel and so disturbing the scattered light that needs to reach the receptor. To reduce this event in the gas flow, a filter to drain the fuel can be implemented.

The gas used is for the first measurements is ambient air, system pressurized to 4-5 bar, the next step is SF6 sulphur hexafluoride for its roughly 5 times higher density then ambient air, 6.075 g/L [22] instead of 1.225 g/L [23]. This is needed to have conditions similar to an actual engine, the higher density enables to pressurize the vessel to a lower pressure with SF6. In a Diesel combustion chamber, peak pressures are 60 - 70 bar [24], to achieve conditions close to a real engine the vessel is not pressurized to 60 bar but only ±10 bar with the use of SF6. Due to setbacks during the building of the setup to perform these measurements there was no time left to implement measurements with the SF6 gas. The air density in the vessel is calculated from the ideal gas law:

$$\rho_{air} = \frac{p\,[Pa].M\,\left[\frac{g}{mol}\right]}{R\,\left[\frac{J}{K.mol}\right].T[°C]} = \frac{4{,}6.10^5.28{,}97}{8{,}31\,.800} = 2{,}003\,\left[\frac{kg}{m^3}\right]$$

Figure 4.1 Tubes with airflow

4. 2. 2. High fuel pressure

To have a better understanding of the injector, spray will be studied at different injection pressures, this work is focused on two specifically, 500 bar and 1200 bar. To operate at different injection pressures, the high pressure pump is driven by an electrical motor. The high pressure pump is feeding pressurized fuel to a control valve mounted on a common rail, the valve is controlled by an electric box called ‘regler’. In the computer is entered a percentage that the control valve is closed, in order to regulate the pressure.

The electric motor has a direct connection to start and stop knob and with an emergency button for when an abrupt stop is needed for safety reasons. A reservoir of fuel is providing fuel to the pump, the pump pressurizes the fuel to the correct value to transport it via a reinforced, flexible line to the common rail. The common rail has a metal line going to the injector and a pressure sensor is mounted on the common rial to confirm the injection pressure right at the injector. The excess fuel is carried from the injector back to the deposit, non-pressurized. The returning fuel is at a higher temperature than before so heats up the deposit, therefore, a cooling system consisting of a heat exchanger that is cooled by fresh water, is added.

Figure 4.2 Build-up High Pressure Fuel Pump

4. 2. 3. Injector signal and trigger

When the injector makes an injection, a trigger is send to the highspeed camera and the BSA processor to start capturing data, the camera starts recording and the BSA Flow processor is receiving a signals from the photomultipliers. To inject click on ‘start cycle’ in the WinDiv software that is controlling the ICU. This software enables helpful settings like injection frequency and the time set to record data in the BSA Flow Software for each injection. A trigger signal from the ICU is send to an electronic device called ‘Magneto’ that generates the exact signal to control the coil lift of the injector, controlled by software program (Solenoid Injector V2) and sets an energizing time of 1500 µs. Injection frequency is set to 1 Hz or 0,5 Hz; the recording time starting from the trigger signal is set to 4ms, these value are entered in the WinDiv software shown in Figure 4.24.

Figure 4.3 Injection Control Unit ICU

Figure 4.4 gives an visual overview to have a better understanding of all non-PDA equipment, how and what type of connections are used are seen in the short legend in Figure 4.4.

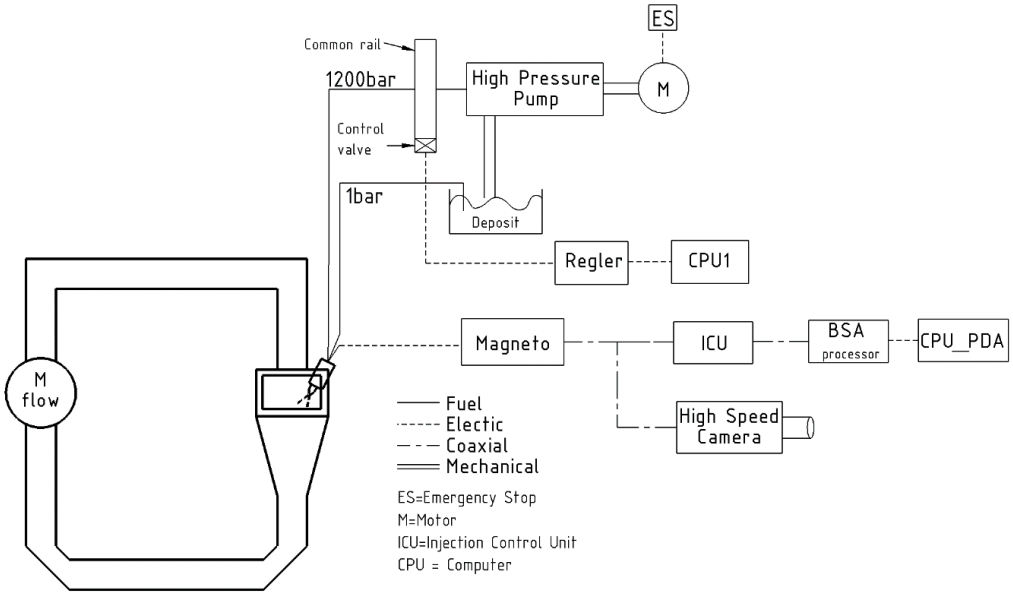

Figure 4.4 Graphical sketch of the Setup

4. 2. 4. High speed camera

In order to have a visual reference between the spray and the probe volume an High Speed Camera is added to the setup. The vessel contains 3 visual accesses where at the left side window the HSC is lined up. The process of an injection is a very quick event at 4 to 10 milliseconds ms [25], to have a representation of the spray this event needs to be split in around 50 frames. This means a picture every $\frac{4\ ms}{50\ frames} = 0{,}08ms$ or $\frac{1\ frame}{0{,}08\ .10^{-3}\ s} = 12500$ frames per second fps are needed.

The FASTCAM SA-X2 is a High Speed Camera system able to capture videos with a framerate of up to 13500 fps at a resolution of 1024x1000 pixels [26]. At these speeds light sensitivity is often the most critical performance criteria. Without high light sensitivity, imaging at high frame rates with short exposure times is not possible therefore, an extra light source directed towards the spray axis is installed. The camera operates via the software Photron FASTCAM Viewer 4, where different settings can be changed. Connecting the camera is via the IP address, then for every trigger the amount of frames to take is e.g. 50 frames, and the resolution is set to 768x768 pixels.

Setting up the camera includes focusing on the spray, this is done by mounting a temporary plastic millimetre paper that represents the plane parallel to the camera and through the spray axis. Because of the reference with the millimetre paper it can be calculated how many pixels there are in one millimetre, for this setup the pixel millimetre factor is 5,62 px/mm.

With the camera can be seen where the probe volume is located in reference to the spray, in Y axis this is easily seen but, in X axis is not straightforward as this is the direction the camera is pointed but still helpful. A second use of the camera is about the localization of the spray, to check if the bisector of the laser beams is perpendicular to the spray axis.

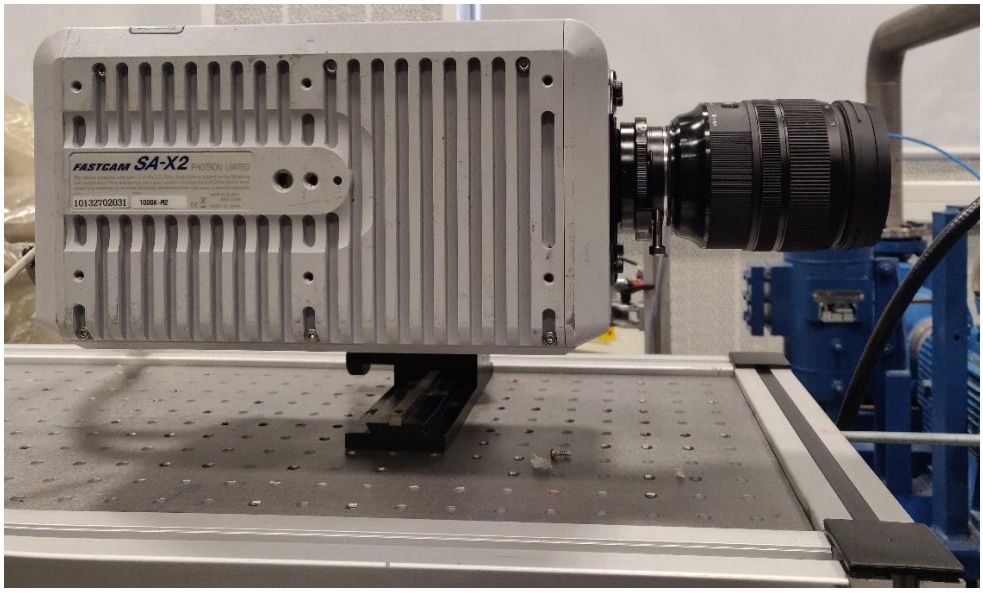

Figure 4.5 High Speed Camera: FASTCAM SA-X2

4. 3. PDA elements

4. 3. 1. Transmitting optic

The laser is of the FlowExplorer family, a powerful Diode Pumped Solid State (DPSS) laser with up to 500mW laser power per wavelength [27]. The wavelength of the laser lines used are 561 nm (yellow) in the horizontal plane and a 532 nm (green), both are first received in a Bragg cell where the initial beam is separated into two equal beams with a frequency difference of 80 MHz between the two.

Figure 4.6 Dantec Dynamics FlowExplorer: Laser

4. 3. 2. Receiving optic

The receiving optic is a FiberFlow Probe 112 mm manufactured by Dantec Dynamics shown in Figure 4.7. The receiving optic is positioned in the forward scattering direction at a scattering angle of 70° mounted on the Travers System, further explained at 4. 3. 4. . Three photodetectors collect the light scattered by single particles passing through the measurement volume.

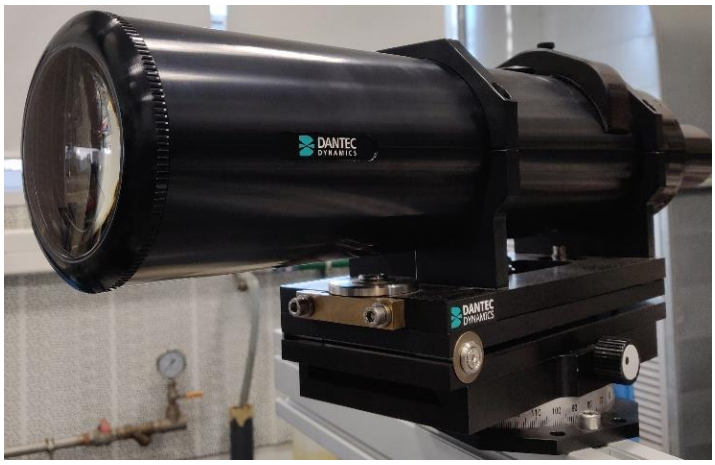

Figure 4.7 Dantec Dynamics FiberFlow Probe: Receiver

4. 3. 3. BSA Flow Processor

The PDA equipment used in this work is PDA system with a Burst Spectrum Analyzer (BSA) F/P Processor manufactured by Dantec Dynamics Figure 4.8. The Processor is connected to the BSA Application software and that is where configuration and monitoring done. The optical configurations are given in Table 4.1. The Dopper bursts are filtered and amplified in the signal processor, which determines f_0 for each particle by frequency analysis, using the robust Fast Fourier Transform algorithm [20].

Wavelength Beam system U1	532 nm
Wavelength Beam system U2	561 nm
Bragg cell frequency (frequency shift)	80 MHz
Receiver type	112 mm Fiber PDA
Scattering Angle	70.0 °
Receiver focal length	310 mm
Scattering mode	Refractive
Particle refractive index	1.440
Medium refractive index	1.000
Beam diameter	1.75 mm
Beam spacing	60 mm
Number of fringes	43
Fringe spacing	U1: 2.798 µm U2: 2.636 µm
Probe volume [mm]	dX: 0.1231 dY: 0.1224 dZ: 1.231
Slit aperture	Pinhole 25 µm Slit 25, 50, 100 & 200 µm

Table 4.1 Optical configurations

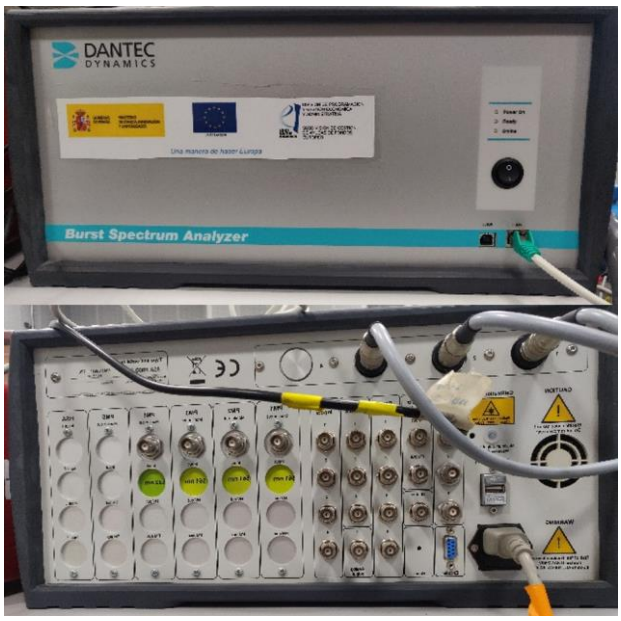

Figure 4.8 BSA Flow Processor

4. 3. 4. Scattering angle

For selecting the scattering there are several factors in play, most preferred is light of the same type with a large amount of energy. Therefore, an angle close to the Brewster angle [28] is desired. The polarisation will happen parallel, in the horizontal plane focused on the 1st order refraction of the light. Between 30° and 70° [20] ensures the dominance of the first mode of refraction. In this project is chosen for the limit at 70° decided by the help tool in BSA Application and what is suited best for the orientation with this vessel. The main parameters for the setup are based on previous papers published on PDPA measurements [29] [30] [31]. These 3 papers utilized a 70° scattering angle and based on other papers [32] [33] it became clear this is the best angle to use for this work and the setup applied here.

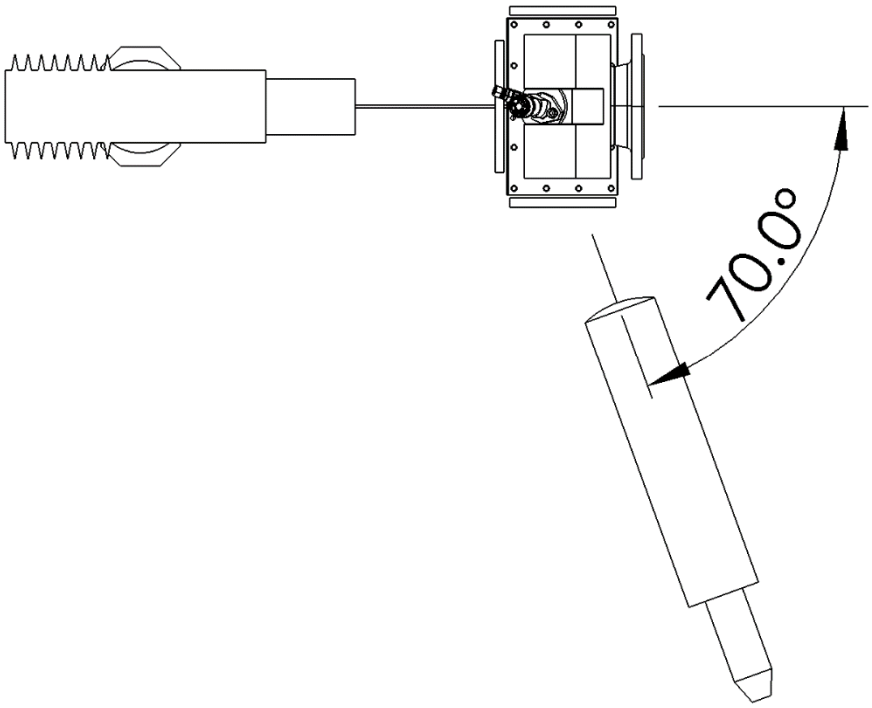

Figure 4.9 Sketch visualisation scattering angle

4. 3. 5. System Monitor

The BSA's on-line system monitor provides immediate feedback on signal quality, data rate, and validation as well as the coincidence between Doppler signals, PM anode current and high voltage. This is a tool for optimizing setup and monitoring of experiments. The System monitor window is opened by right-clicking on the BSA Application icon in the project explorer and selecting System monitor from the drop down list.

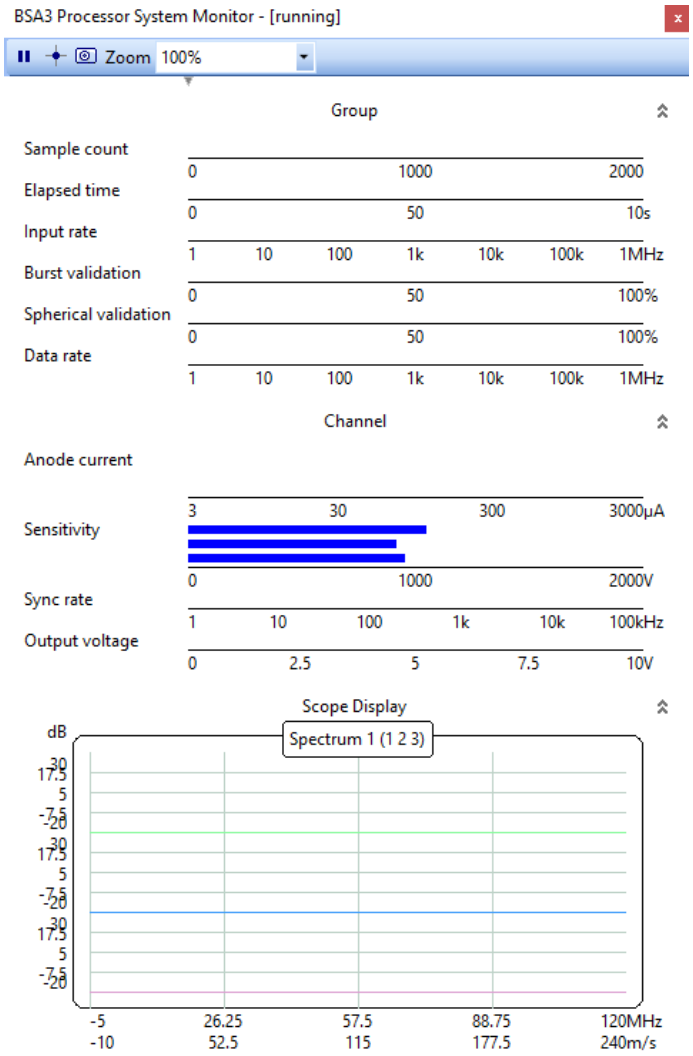

Figure 4.10 Screenshot System Monitor

Sample count	The maximum samples number is a stop criterion for data acquisition for the selected coincidence group
Elapsed time	The time it is recording data at one position, resets when it is at a new position. Maximum acquisition time stops data acquisition for the selected coincidence group.
Validation	Is an indicator for a good Doppler burst
Data rate	Amount of samples that are measured, this is preferred high value
Anode current	Anode current shows the mean photo-multiplier output current. The scale is fixed with 3 mA as maximum.
Sensitivity	It sets the high voltage to the photo-multiplier. Optimization should take Signal gain into account, the criterion may be a compromise between validation rate and the data rate. Set around 1000 V.
Scope display	The Scope Display shows digitized bursts or their associated spectrum on-line. The Scope display shows the full burst, and dotted vertical lines in the display indicate which part is being analysed, and is set to ‘Bust Signal’.

4. 4. Spray orientation

The injector tip contains 4 holes from which comes along 4 sprays, one of these sprays is studied in this project, called the spray of interest. It is important that the spray (axis) of interest is parallel to the traverse system with the aim to simplify the coordination within the spray. To centre the probe volume on the spray axis, at the nozzle tip, an undoubtable localisation of the spray must be known. This process is done via different approaches that need to lead to the same result, for that reason it is split into 4 parts: SolidWorks model, millimetre paper, front face center punch, and windows mounted (Snell's law)

4. 4. 1. SolidWorks model

SolidWorks is a Computer Aided Design CAD tool that helps to determine certain distances. Some parts like the injector and the head of the vessel are parts that already existed. The vessel, windows, metal frames, laser with beams, receiver and travers system were not available as a 3D part, therefore, the dimensions of these parts had to be measured in the lab and were then drawn in 3D SolidWorks environment. All parts are positioned together with the necessary mates to become a virtual 3D assembly model comparable to the real setup. This is particularly useful for finding dimensions that are not possible to measure correctly on the setup itself, example shown in **Figure 4.11**.

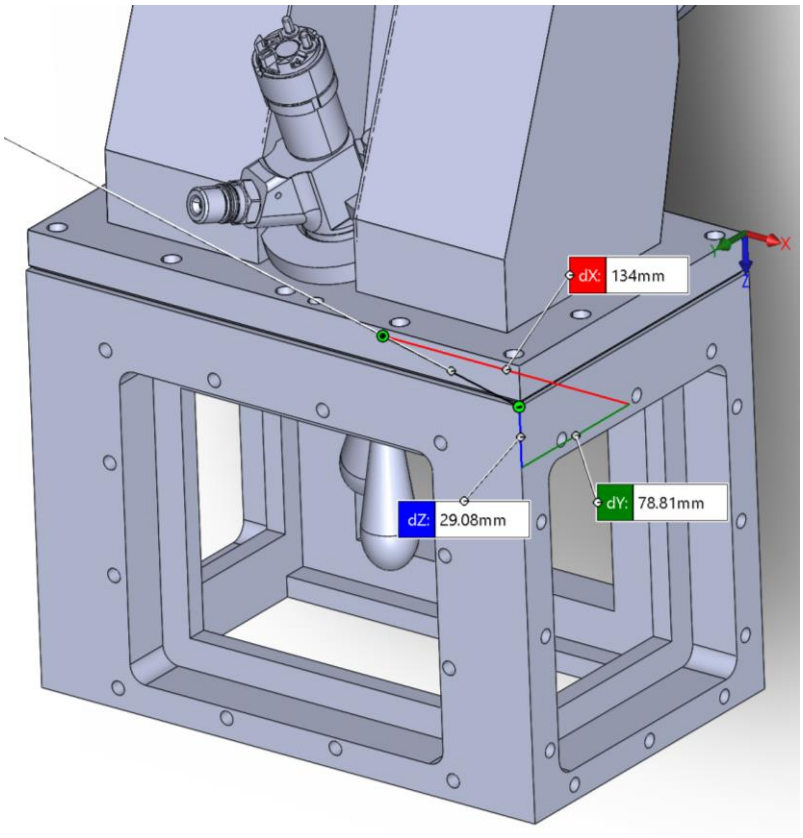

Figure 4.11 SolidWorks model with measuring tool

4. 4. 1. Orientation of the injector

Throughout this document, a comparison to a supposed axis is often made to indicate the direction in which the spray is going, or the travers system is moving. In order to avoid misunderstandings, a clear explanation with visual support is provided, using X Y and Z axis that correspond to the X Y and Z axis of the traversing system on which the optical equipment is mounted. The traverse system and the vessel are arranged parallel to each other to facilitate coordination. Standing in front of the traverse system, one moves from right to left is the positive X axis, from front to back is the positive Y axis and from top to bottom is the positive Z axis, seen visually in Figure 4.12.

The Cummins injector has 4 orifices that provides 4 sprays, one of which we will study, called the spray of interest, marked in blue in Figure 4.12. The spray of interest is vertical, follows the Z axis and is positioned closest to the front window for the best possible optical access.

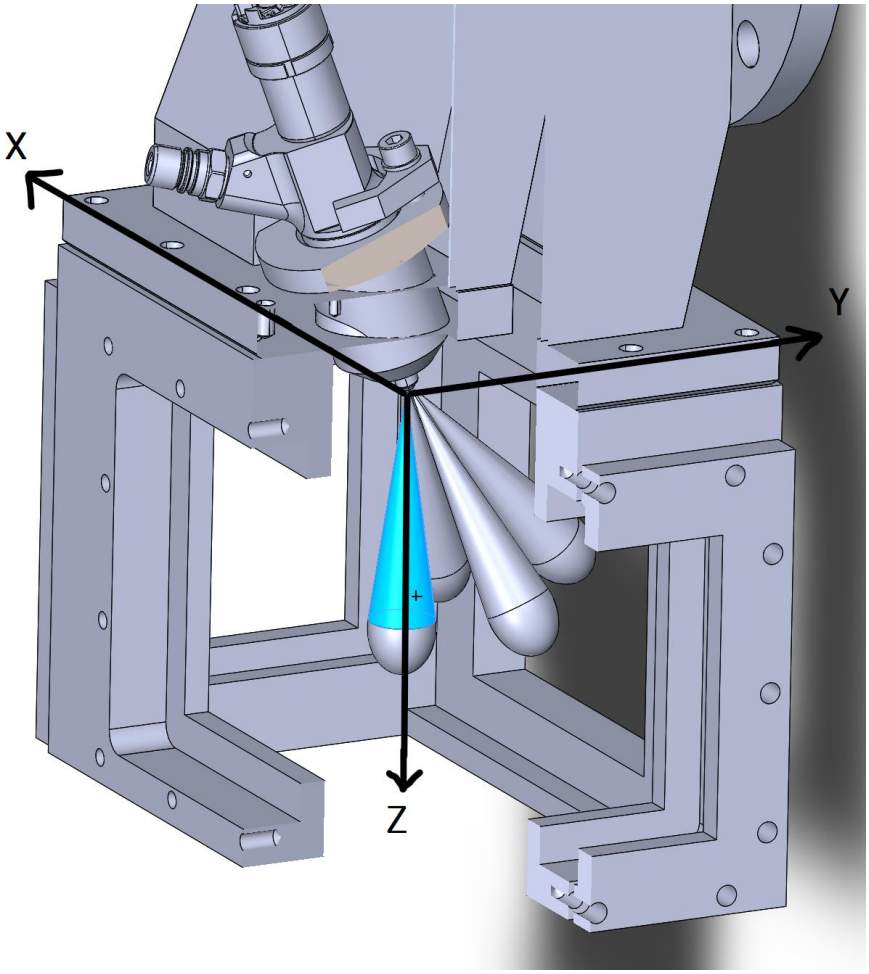

Figure 4.12 Vessel explanation XYZ axis

4. 4. 2. Millimetre paper

The injector is placed in an adaptor piece that is welded into the head of the vessel, how the injector is mounted in the head of the vessel decides how parallel the spray axis is to the traverse system. To confirm both are parallel it is a step by step process, first check if the spray axis is parallel to the vessel itself, then if the vessel is parallel to the travers system. To review whether the spray is vertical in the vessel, the configuration in Figure 4.13 is made at 8 Z-positions to track the spray. Z-positions are distances defined from the nozzle tip and are the following: 20, 25, 30, 40, 50, 60, 80 & 100.

For each position 2 papers are used, ones the millimetre paper is installed a mark is made on the paper at the right and left side of the vessel. For each paper between one and three injections are made until the paper is penetrated with a hole remaining. When the paper is removed a X and Y coordinates that identify the location of the spray axis are obtained and the result is given in Figure 4.14 & Figure 4.15. Since the marked reference on the paper is done by hand as accurate as possible still a 1 mm uncertainty is given, therefore, we consider the spray axis vertical, parallel to the vessel.

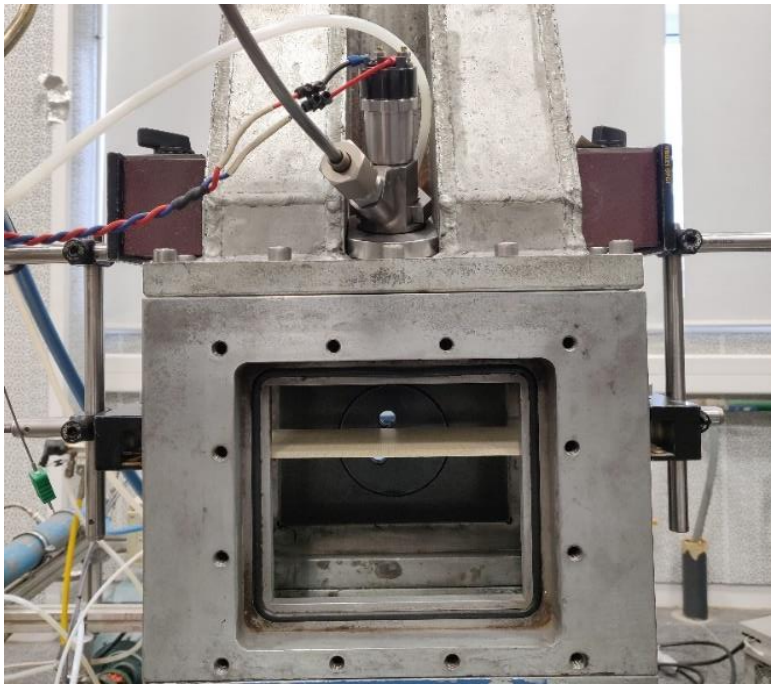

Figure 4.13 Configuration millimetre paper at different heights

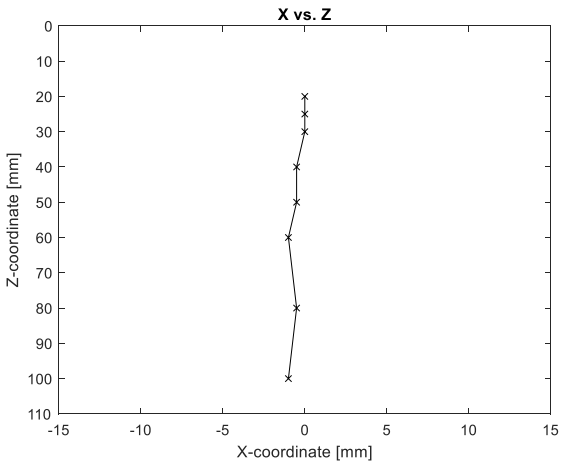

Figure 4.14 Track spray axis X vs. Z

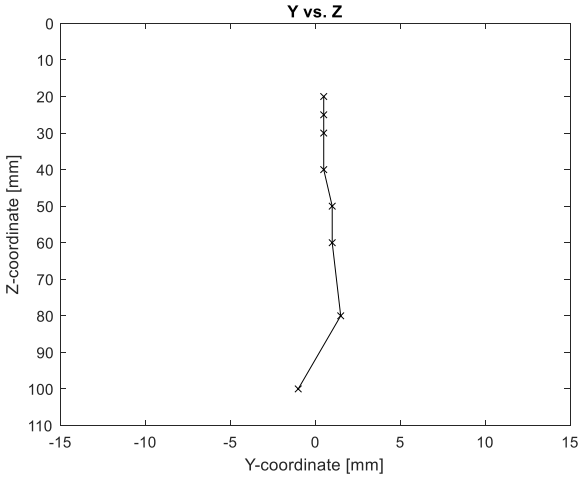

Figure 4.15 Track spray axis Y vs. Z

4. 4. 3. Relate two coordinate systems

The closed system of tubes, where air is flowing through, has one flexible tube seen in Figure 4.1. When the system is pressurized to 4 bar the absolute position of the vessel is different due to the flexible tube that can expand. To register this change in location two center punches at in the front face of the vessel are created, two points are made to increase accuracy. With the not-pressurized system the measurement point of the laser is positioned at one point then, the system is pressurized and the laser is relocated. The relative change in position of the vessel is now known. The center punch point always has the same distances to the injector tip, these coordinates form center punch to the injector tip are carefully noted down. This enables to easily relocate when equipment moved positions since the center punch is an easy accessible point with the laser.

4. 4. 4. Parallelism between window axis and transmitter axis

When in full operation the laser beams travel through 3 different mediums before they intersect and form the probe volume: ambient air, methacrylate window, and pressurized air. Since the behaviour of light depends on the medium it travels in, known as Snell's law, a change in location of the probe volume is expected due to the mounting with and without the windows. Snell's law says the speed of light and the direction changes on the medium it travels in [34]. This difference is observed by mounting a small metal plate in the XZ plane of the vessel, on the metal plate mm paper is glued. The laser is positioned on multiple points on the paper and coordinates are noted down, without windows mounted. After the same process is executed but, with the windows mounted to detect any differences. This process is done for both horizontal laser, seen in Table 4.2 and vertical laser seen in Table 4.3. The main direction of the laser beams are in Y, therefore, the largest change in location of the probe volume detected is in Y, namely 14,7 mm. For the Z coordinate there is also a difference but not significant and since the accuracy in Z position is not as crucial for measurements will this be accepted.

Horizontal Laser		
X	**Y**	**Z**
0	14.5	-0.7
0	14.5	-0.7
0	14.5	-0.7
0	15.0	-0.5
0	15.0	-0.5
0.2	15.0	-0.5
0	14.5	-0.6
Average: 0.03	14.71	-0.60

Table 4.2 Difference in location probe volume by Snell's law horizontal laser

Vertical Laser		
X	**Y**	**Z**
0	14.5	-0.5
0	14.5	-0.5
0	14.5	-0.5
0	15	-0.5
0	15	-0.5
0.2	15	-0.5
0	14.5	-0.6
Average: 0.03	14.71	-0.51

Table 4.3 Difference in location probe volume by Snell's law vertical laser

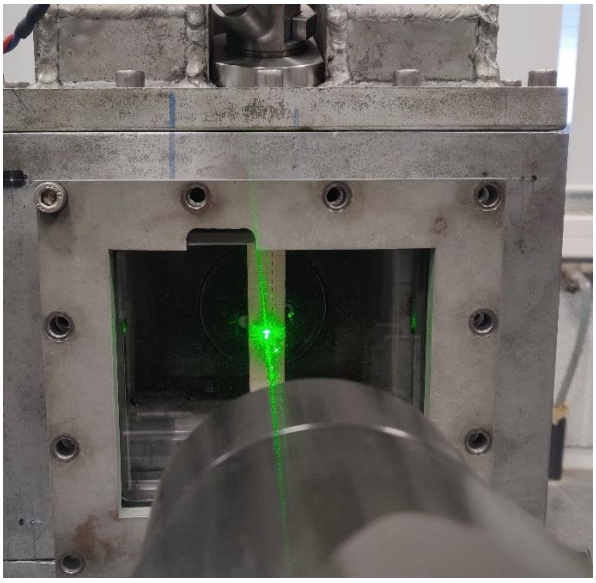

Figure 4.16 Laser point without windows

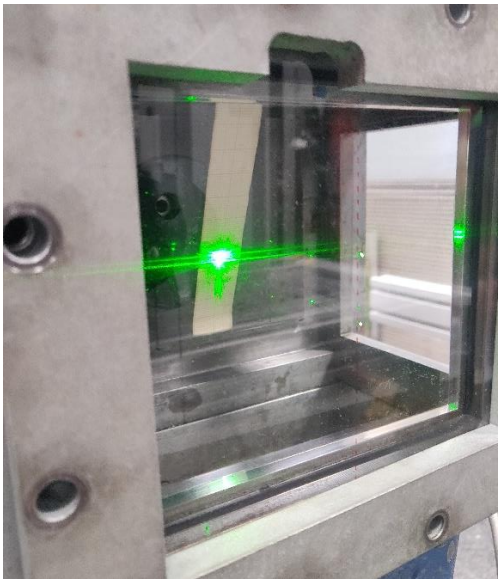

Figure 4.17 Laser point with windows

4. 4. 5. 3D Velocity map

The density in these conditions with air are not comparable to the one in a real engine, therefore the use of SF6 is needed. Before executing measurements in this gas a reference of the injection spray needs to be determined. Consequently, velocities are obtained throughout the spray following a X map, Y map and diagonal XY map. For each position an average of the five highest velocity values is taken to eliminate extreme values. Every velocity has an X and Y coordinate, a 3D graph is constructed via MATLAB by interpolating between the known points. Coordinates are chosen in steps of one millimetre and close by the spray axis steps of half a millimetre, in the plane perpendicular to the spray axis. This process is done at three Z distances namely Z50, Z70, and Z90 millimetre from the nozzle tip.

Configuration: **Pr470 CP4.6 Pinhole25 Z50**

Velocities at Z50

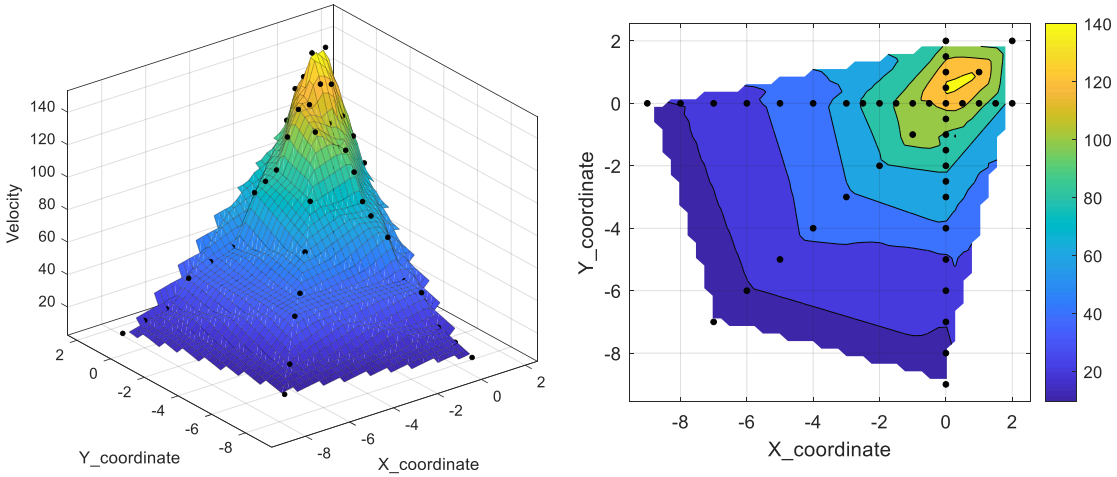

Velocities at Z70

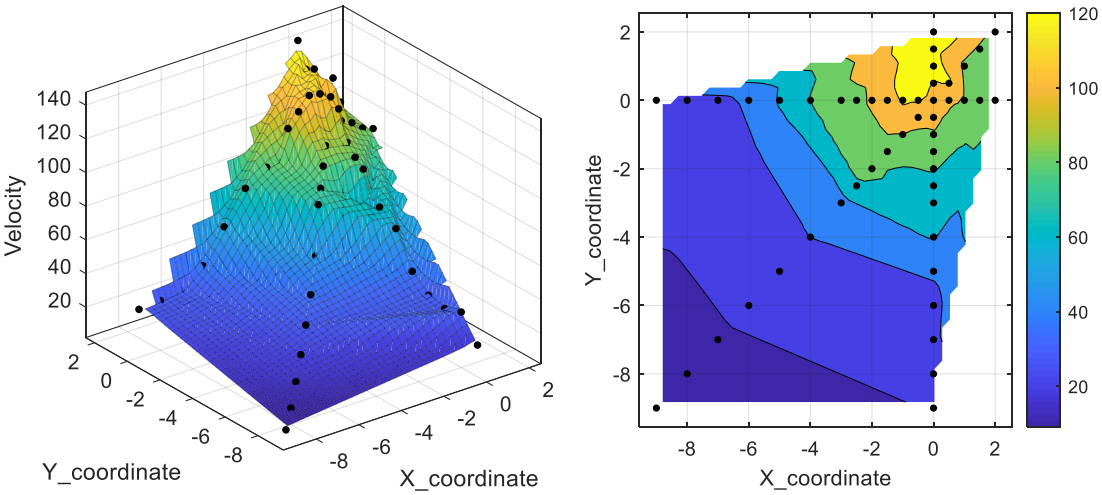

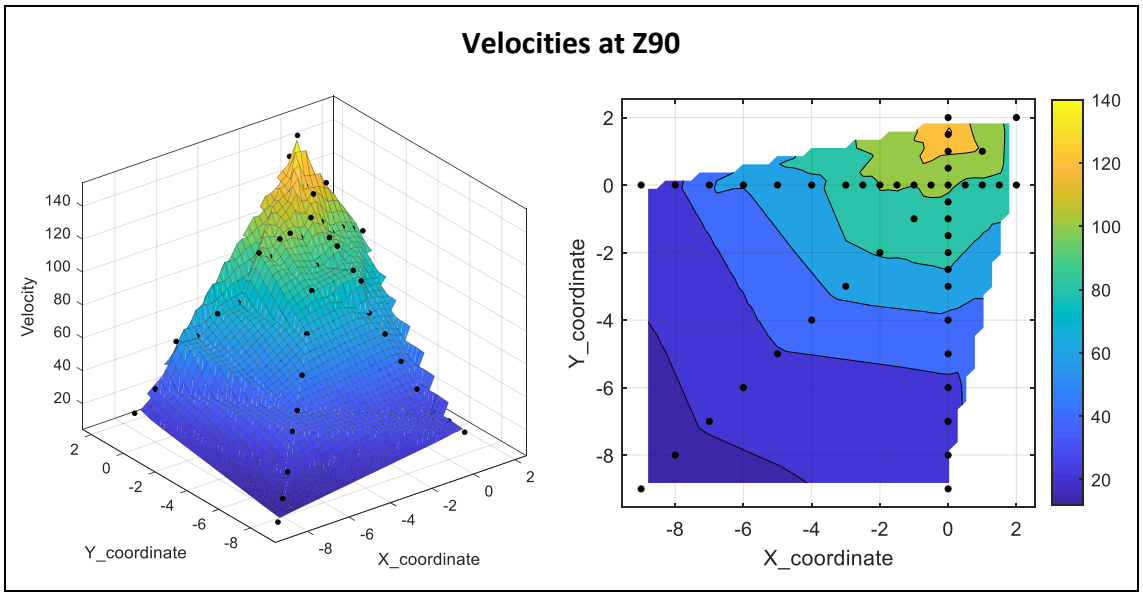
Velocities at Z90
Velocity
Y_coordinate
X_coordinate
Y_coordinate
X_coordinate

4. 5. Acquire PDA data

Start with to following assumptions:

- Optics and the traverse system have been configured
- 80 MHz Bragg cell is used
- All cable connections have been made
- The laser is running
- The transmitting optics and receiving optics are precisely aligned

1. Start the BSA Flow software on the computer and create a New Project in the dialog box
2. Connect to the BSA Flow Processor and open the System Monitor when connected, more info about System Monitor in section 4. 3. 5. System Monitor
3. In the BSA Application window, a tree structure including icons 'Processor, Group 1, LDA1, PDA2, PDA3, LDA4 and Optical PDA System' appears. Clicking on one of the icons will display its properties. 2D PDA Non-Coincidence is selected, in this setting the data is separated in Group1 and Group2, therefore, the data from LDA4 (horizontal velocities) does not need to equate to Group1.

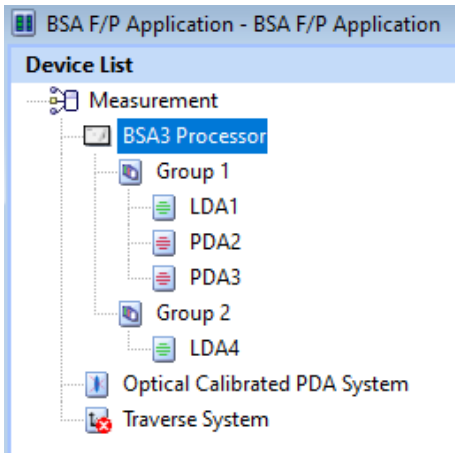

Figure 4.18 BSA Application Device List

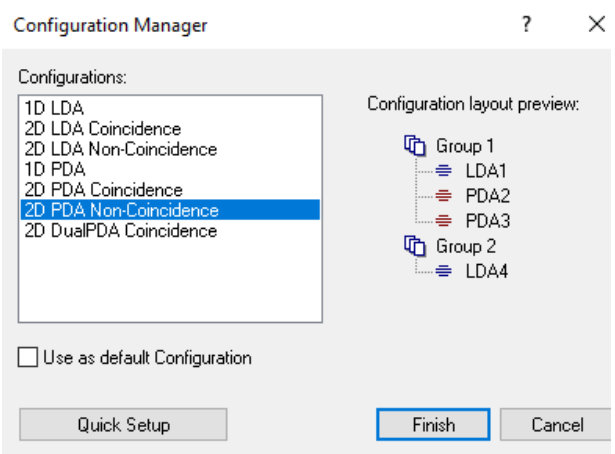

Figure 4.19 Configuration Manager: 2D PDA Non-Coincidence

4. In the BSA Application window click on Processor. The Processor properties are common for all velocity channels in the processor. In the property editor, for the User interface property select 'Normal'. This will show the normal properties for the Processor, Group1 and LDA1, sufficient for most applications. The Advanced user interface shows an extended list of properties. Data collection mode is set to 'Burst', is used when high temporal resolution is required.

5. In the BSA Application window click on Group 1. The Property Editor shows the Stop criteria. Here are the stop criteria set to: Max. samples to 10000 and Max. acquisition time to 100 seconds. Group 2 is set: Max. samples 10000 and Max. acquisition time to 50 seconds.

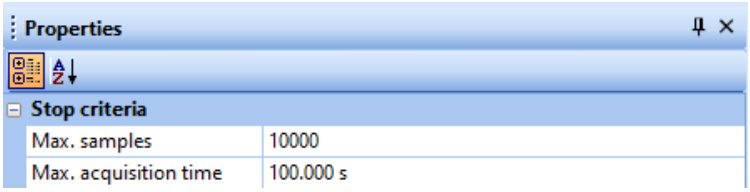

Figure 4.20 Properties: Stop criteria

6. LDA 1 properties are specific to velocity channel 1, at the Range and Gain list properties are the Center velocity and Velocity span values depending on the optical properties, for Group 1: corresponding 269 m/s and 586 m/s, for Group 2: 0m/s and 22m/s.

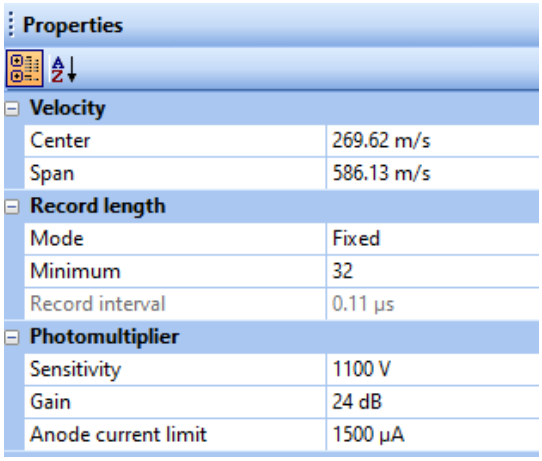

Figure 4.21 Properties: Velocity and Sensitivity Group1

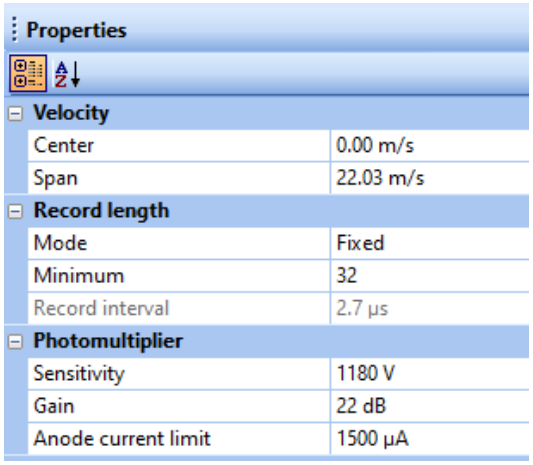

Figure 4.22 Properties: Velocity and Sensitivity Group2

7. Sensitivity level must be carefully set, depending on the Data Rate. In operating setting 'Repetitive' is injected and started from a low sensitivity level 500V, then go up with Laser power and notice differences in the system monitor, lower Laser power again and start over with a higher e.g. 600V sensitivity level. Follow this process until a high 'Data Rate' and 'Coincidence' is reached but, avoid overloading the photo-multipliers. In this work sensitivity levels were between 950 V to 1200 V depending on the operating conditions seen in Figure 4.21 & Figure 4.22. Optimize data rate and validation by adjusting the sensitivity and gain settings under the 'Range and Gain' properties.

8. Optical PDA properties include Beam system U1, Beam system U2, PDA receiver, particle, and medium properties. Defining of the optical PDA properties is explained at 4. 3. PDA elements

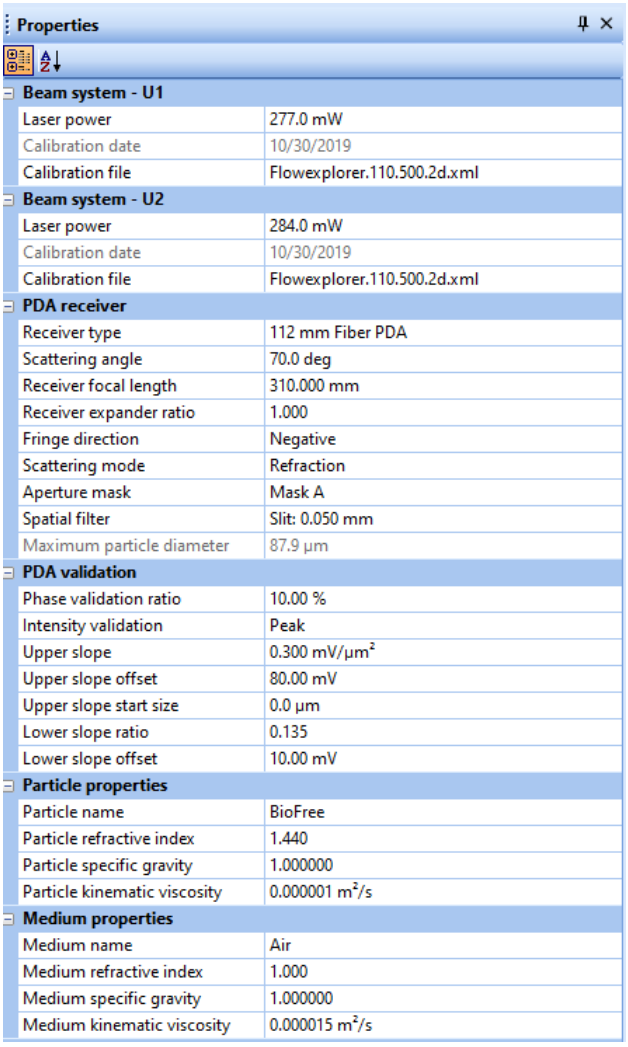

Properties

Beam system - U1	
Laser power	277.0 mW
Calibration date	10/30/2019
Calibration file	Flowexplorer.110.500.2d.xml
Beam system - U2	
Laser power	284.0 mW
Calibration date	10/30/2019
Calibration file	Flowexplorer.110.500.2d.xml
PDA receiver	
Receiver type	112 mm Fiber PDA
Scattering angle	70.0 deg
Receiver focal length	310.000 mm
Receiver expander ratio	1.000
Fringe direction	Negative
Scattering mode	Refraction
Aperture mask	Mask A
Spatial filter	Slit: 0.050 mm
Maximum particle diameter	87.9 µm
PDA validation	
Phase validation ratio	10.00 %
Intensity validation	Peak
Upper slope	0.300 mV/µm²
Upper slope offset	80.00 mV
Upper slope start size	0.0 µm
Lower slope ratio	0.135
Lower slope offset	10.00 mV
Particle properties	
Particle name	BioFree
Particle refractive index	1.440
Particle specific gravity	1.000000
Particle kinematic viscosity	0.000001 m²/s
Medium properties	
Medium name	Air
Medium refractive index	1.000
Medium specific gravity	1.000000
Medium kinematic viscosity	0.000015 m²/s

Figure 4.23 Properties: Optical PDA

9. Set the recording time for each injection in the WinDiv software (that controls the Injection Control Unit ICU), first at a higher value to make sure data is acquired, then lower it to where data is relevant, in this work recording time is set to 4000 µs.

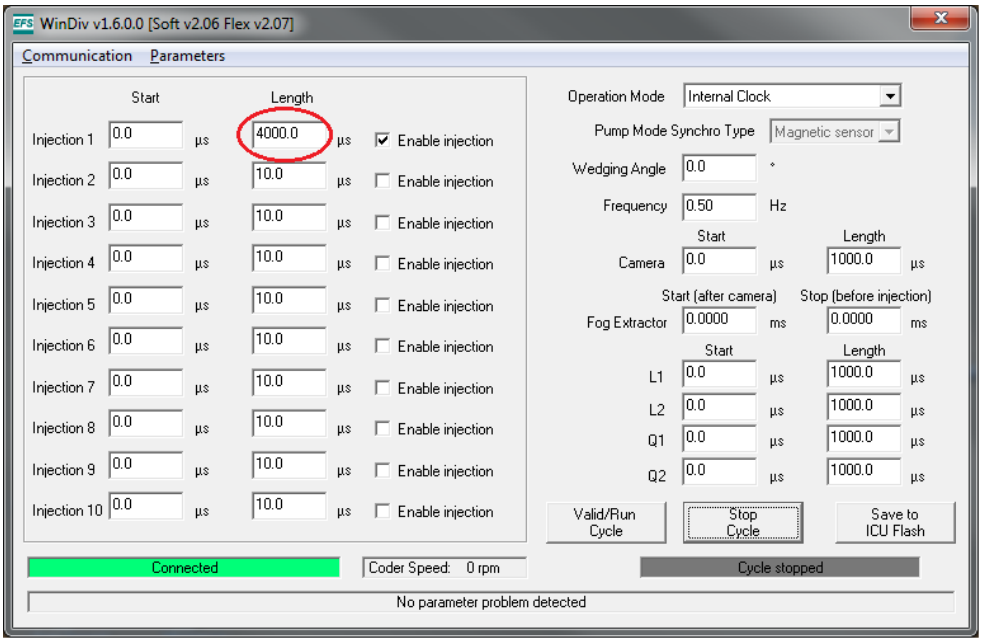

Figure 4.24 WinDiv Software

10. To display a velocity and a diameter distribution plot, right-click on the BSA Application icon in the project explorer and select New. First select Cyclic phenomena from the dialog, this is done because the data from multiple injections are shown on the same plot to acquire 10000 samples. Then a second object 2D Plot is added under the Cyclic phenomena. A new window appears in the workspace. The 2D Plot needs to be configurated to what parameters want to be displayed on X and Y axis of the plot, options are: arrival time, transit time, time, cycle No, bin class velocity U, phase U12, phase U13, diameter, time bin, count, velocity U mean, velocity U rms, phase u12 mean. If the 2D Plot is not showing the data you expected, you can add the object 'List' where you see all samples collected in a list with numbers of the parameters.

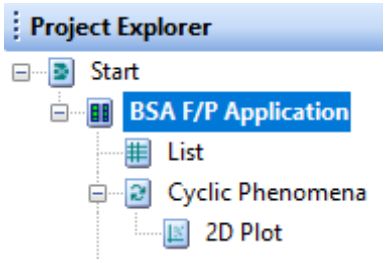

Figure 4.25 Object: Cyclic Phenomena, 2D Plot

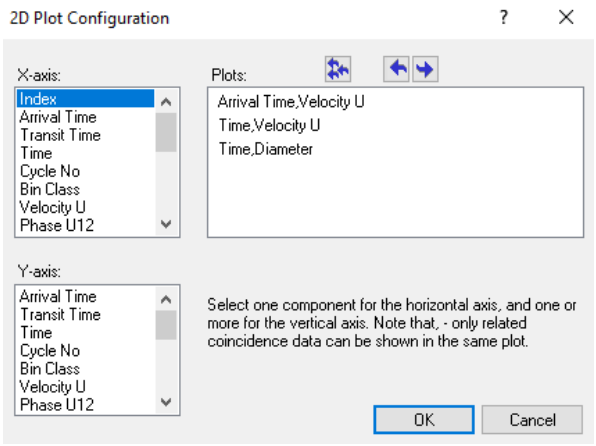

Figure 4.26 2D Plot Configuration

11. To acquire data in multiple positions at ones, in the “BSA Application Window tab Measurement Positions, coordinates are entered.

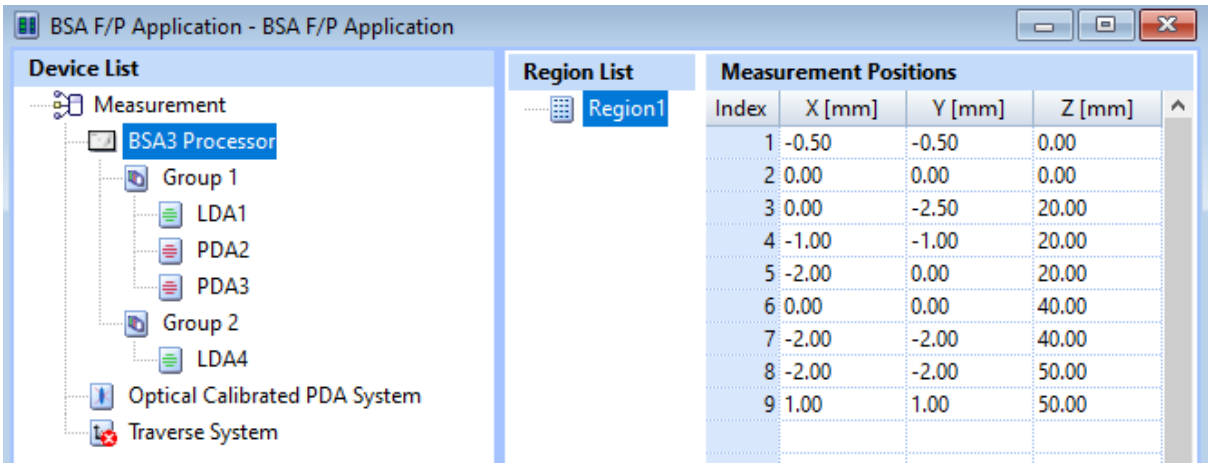

Figure 4.27 Measurement Positions

12. To start acquisition, click on BSA Application in the project explorer, and click on the Run button in the tool bar and when multiple positions are entered, you also have to click ‘Acquire all positions’. Then the PDA system is waiting for particle to pass by in the flow, therefore, clink ‘Run Cycle’ in the WinDiv software shown in Figure 4.24, the injector starts injecting. The 2D Plot will be updated during the measurements. The update rate depends on the data rate. With high data rates and a large number of samples, you will see several updates during an acquisition. When one of the stop criteria (Max. samples or Max. time) is fulfilled the Travers System automatically moves to the next position and the 2D Plot is reset.

13. When the acquisition is completed, the "Run" button is clear again. If the System monitor is open, either the Samples or Acquisition bar graph is at full scale. Under the menu "Tools - Options - General" you can select "Feedback with sound". With this option active, you will hear a beep from the PC when acquisition is completed at one location before it moves on to the next one. To save the data, click the Save button in the toolbar (or select File-Save in the menu bar)

14. For easier use of the data, the collected data is exported to a ‘.txt’ file, which is used for analysis in MATLAB. To obtain the ‘.txt’ file an New object under BSA F/P Application is made, called Export. Here is set where to save the files and what headers with information to add to the file, then right click on the object export and select Run. The data is now save in a .txt file at the given location in the PC for further analysis.

CHAPTER 5. RESULTS AND DISCUSSION

5. 1. Measurement configurations

To get to a better understanding of the new PDPA equipment measurements in different operating conditions are compared to determine how parameters effect the measurement. The results published here are all done with the configuration given in Table 5.1 unless given otherwise in the graph. For all measurements the vessel is pressurized with air, therefore, conditions are not completely similar to those of an actual engine. The air density in the vessel is calculated in 4. 2. 1. Flow in system.

The position where the measurement was carried out is given in cartesian coordinates at the top in the graph in the order x-coordinate; y-coordinate; z-coordinate. The [0; 0; 0] reference position is 30 mm below the injector nozzle as this is the closest position accessible with the laser. All measurements are done in the following conditions unless mentioned differently.

Pinj	470 - 1200 [bar]
Air density @ 4.6 bar	2.003 [kg/m³]
Energizing Time ET	1500 µs
Injector nozzle diameter	250 µm

Table 5.1 Basic injection configuration

5. 2. Comparing: injection pressure & Z location

In following graphs 4 different Z locations are compared, at 470 bar (left column) and 1200 bar (right column). At the lower pressure there are significantly more samples measured at higher velocities considering that at 1200 bar the droplets are moving faster and are therefore more difficult to measure. This is seen that between 2 ms and 3 ms little samples are registered. While moving away from the nozzle velocities drop at 470 bar, but at 1200 bar higher velocities are registered further from nozzle, because, the spray is too dense liquified close to the nozzle tip.

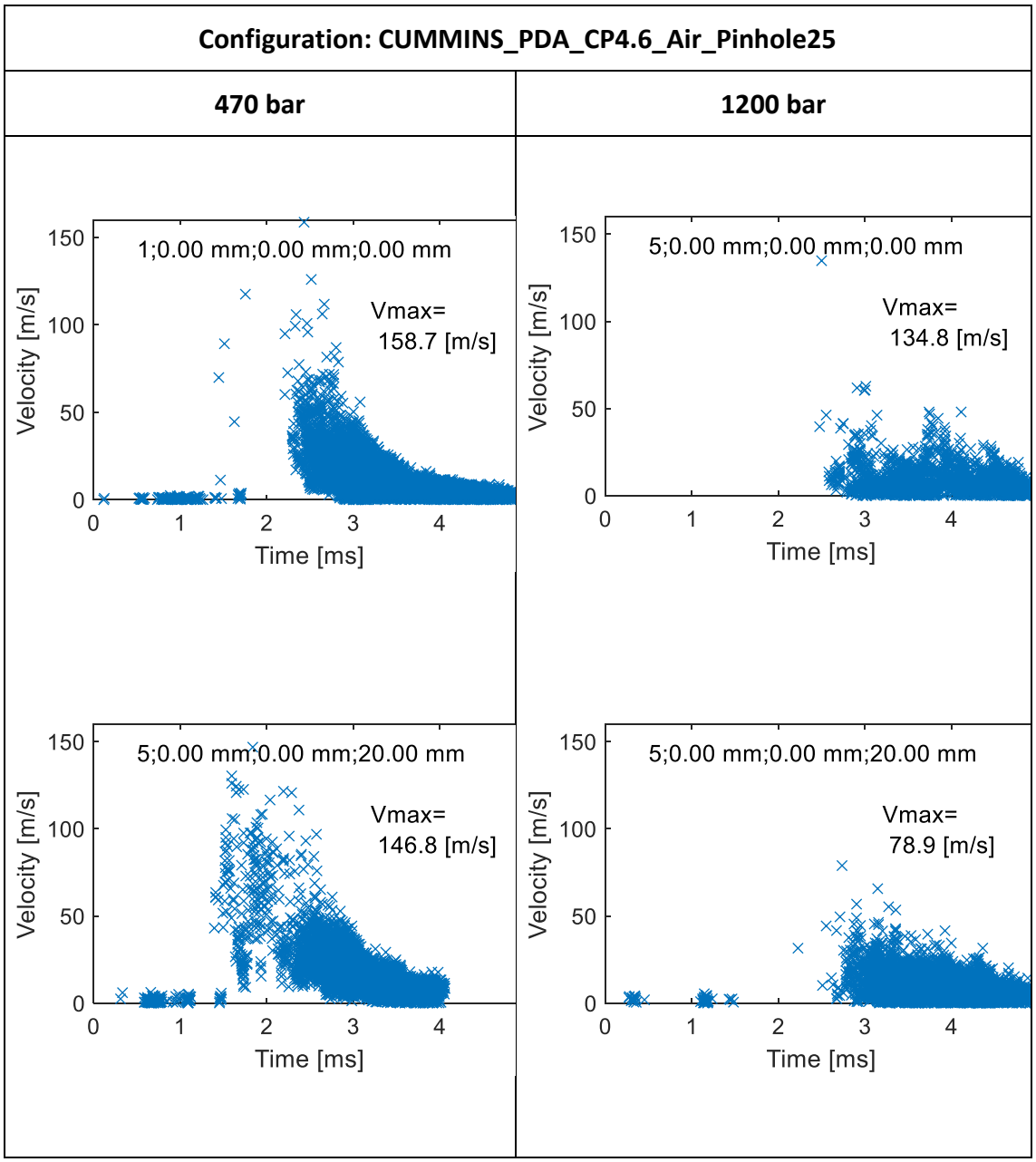

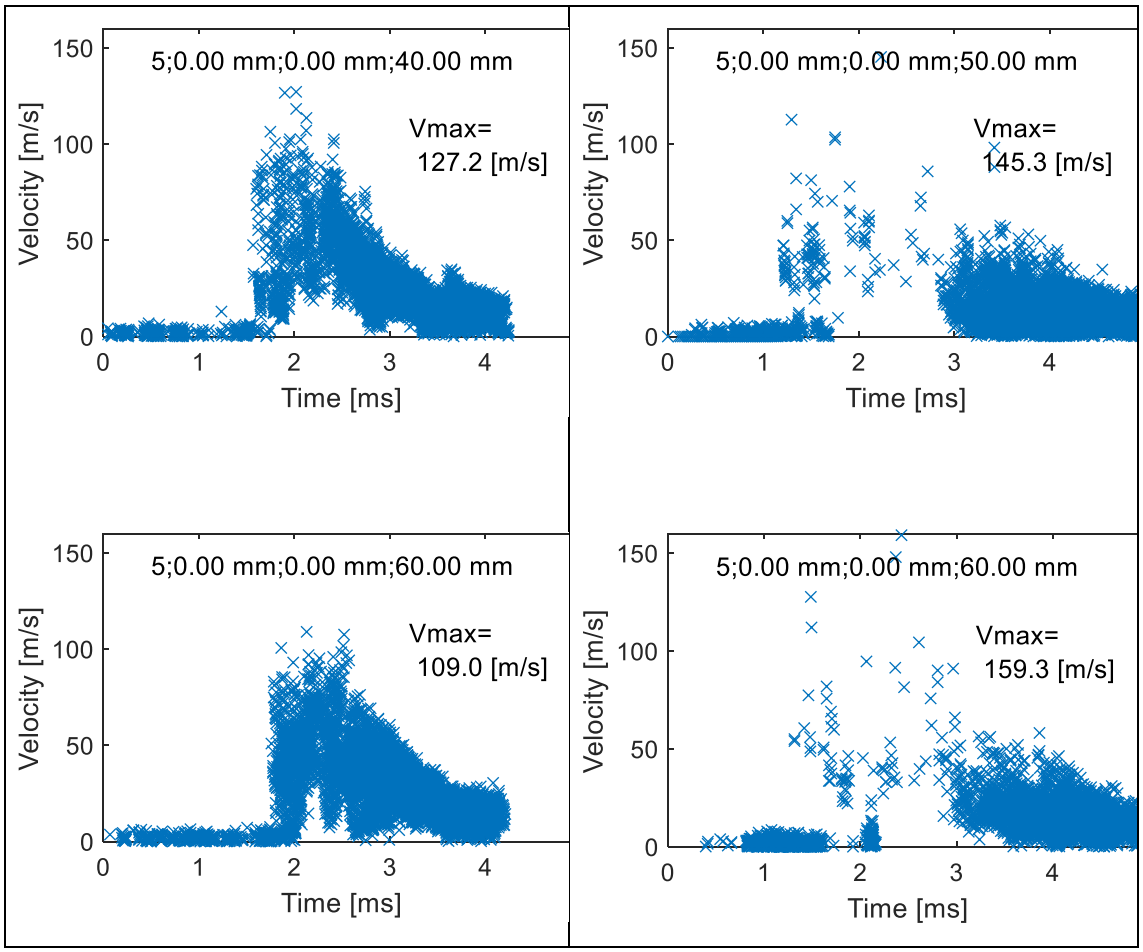

5. 3. Comparing Slits

The “slit aperture width” in the receiver affects the size of the measuring volume in which particles are detected. Expanding the slit aperture means less acquisition of validated droplets as there is more chance that two droplets pass through the control volume at the same time [29]. Contracting the slit aperture means more validated droplets, however, the droplets with higher velocities could be missed. Those droplets are responsible for the highest velocities on the spray axis. Next to different slit there is the pinhole, a circular shaped aperture that was a trustworthy balance between amount of samples and velocities values.

Configuration: **Pr 1200; CP4.6 bar**

Slit 50 100, 200 & Pinhole 25

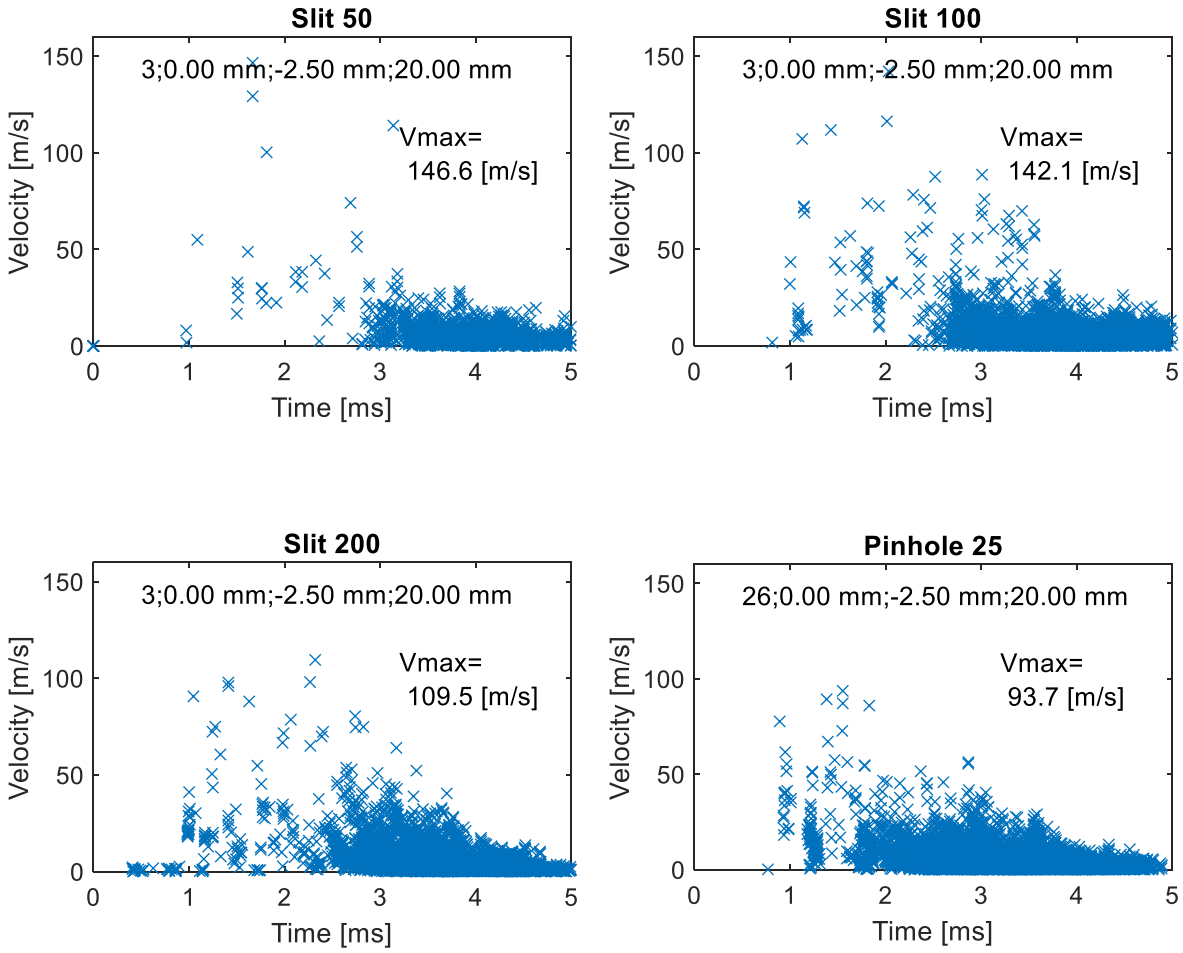

Configuration: **Pr 470 CP4.6 bar**

Slit 50 & Slit 200 at 2 positions

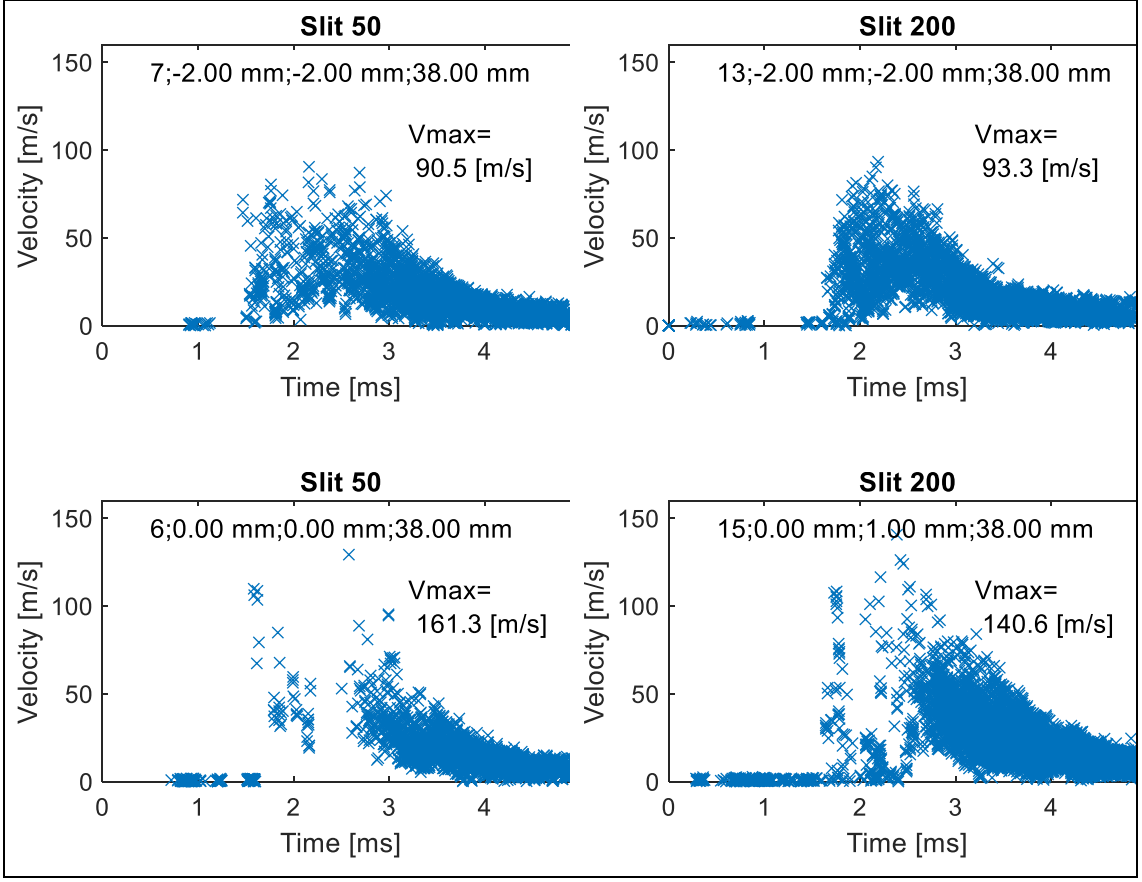

Using the Pinhole 25 aperture width was able to register the higher velocities, therefore, this gives preference to perform measurements with. Doing so at the lower pressure 470 bar brought along a more visible velocity profile (left graph) and at 1200 bar the peak velocity values were missing. Expected is that the faster droplets are smaller and as a result harder to measure.

Configuration: **CP4.6 Pinhole25**

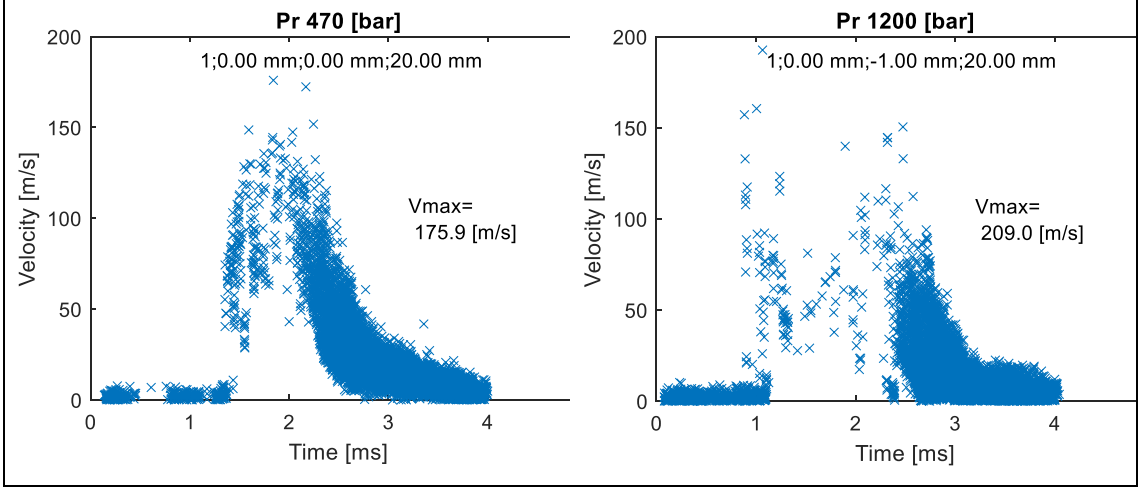

5. 4. Conclusion

Throughout this work, I have tried to provide a detailed explanation of how the PDA technique works and the steps that must be followed to assemble and use it correctly. Finally, I have tried to give a series of results, giving as much information as possible about the conditions under which they were obtained, so that, if desired, the most accurate possible comparison can be made. Despite all the developments and improvements that have taken place in the course of this work, there are still aspects that can be improved. Perhaps the most obvious is the addition of a filter in the system that removes liquid particles from the flow that, after a series of injections, is filled with suspended particles that circulate for a long time, preventing the refracted light from reaching the receiver. In order to clarify how the settings affect the results, further measurements need to be made. So far, this has been difficult as different settings and locations in the spray have been carried out but not consistently to see how one variable effects the measurement. It is often an composition of multiple parameters adjusted to each other to bring along the best result.

REFERENCES

[1] H. Z. C. Y. Yeh, Localized fluid flow measurements with an He-Ne laser spectrometer, Colombus: Applied Physics Letters, 1964.

[2] K. S. Klaus Mollenhauer, "History and Fundamental Principles of the Diesel Engine," in *Handbook of Diesel Engines*, Berlin, Heidelberg, Springer, 2010, pp. 3-30.

[3] Capital Reman Diesel Engines & Engine Parts, "The History and Mysterious Death of Rudolf Diesel," 21 July 2017. [Online]. Available: https://www.capitalremanexchange.com/history-death-rudolf-diesel/. [Accessed 20 November 2021].

[4] K.-H. Dietsche, "History of the diesel engine," in *Fundamentals of Automotive and Engine Technology: Standard Drives, Hybrid Drives, Brakes, Safety Systems*, Wiesbaden, Springer Fachmedien Wiesbaden, 2014, pp. 8-17.

[5] K.-H. a. K. D. Dietsche, "History of the automobile," in *Fundamentals of Automotive and Engine Technology: Standard Drives, Hybrid Drives, Brakes, Safety Systems*, Wiesbaden, Springer Fachmedien Wiesbaden, 2014, pp. 1-7.

[6] J. H. Y. W. Z. W. Z. L. Y. Z. H. W. X. B. J. Hao, "Real-world fuel efficiency and exhaust emissions of light-duty diesel vehicles and their correlation with road conditions," *Journal of Environmental Sciences,* vol. 24, no. 5, pp. 865-874, 2012.

[7] European Environment Agency, "Greenhouse gas emissions from transport in Europe," European Environment information and Observation Network, 18 Nov 2021. [Online]. Available: https://www.eea.europa.eu/ims/greenhouse-gas-emissions-from-transport. [Accessed 1 Dec 2021].

[8] European Parliament, "Greenhouse gas emissions by country and sector (infographic)," in *News European Parliament*, Brussels, 2021.

[9] European Parliament, "CO2 emissions from cars: facts and figures (infographics)," in *News European Parliament*, Brussels, 2019.

[10] I. Z. Péter Nagy, "A Review on the Differences Between Particle Emission, Filtration and Regeneration of Particulate Filters of Diesel and Gasoline Engines," in *Vehicle and Automotive Engineering*, Singapore, Springer, Singapore, 2020, pp. 158-173.

[11] C. H. Frederik Van Den Broeck, Verbrandingsmotoren 2 Basis Diesel, Kortrijk: Vives, 2016.

[12] A. Schmid, “Experimental characterization of the two phase flow of a modern, piezo activated hollow cone injector,” Researchgate, Winterthur, 2012.

[13] L. E. Drain., The Laser Doppler Technique, Harwell: Atomic Energy Research Establishment, 1980.

[14] P. R. M. Kleuskens, Laser Doppler anemometrie: volgens het backscatter, fiber optics principe, Eindhoven: Technische Universiteit Eindhoven, 1992.

[15] V. Uruba, “Measurement of Flow Velocity,” Czech Technical University Prague, Prague, 2021.

[16] Dantec Dynamics, BSA Flow Software User Guide v6.50, Skovlunde, Denmark: Not public, 2017, p. 536.

[17] C. J. Bates, “ANEMOMETERS (LASER DOPPLER°,” Thermopedia, Cardiff, 2011.

[18] C. J. Bates, “Thermopedia Anemometers (Laser Doppler),” 2 February 2011. [Online]. Available: https://thermopedia.com/content/558/. [Accessed 23 December 2021].

[19] W. Bachalo, “Experimental methods in multiphase flows,” *International Journal of Multiphase Flow,* vol. 20, no. 1, pp. 261-295, 1994.

[20] Dantec Dynamics, “Measurement Principles of PDA,” December 2019. [Online]. Available: https://www.dantecdynamics.com/solutions-applications/solutions/spray-and-particle/phase-doppler-anemometry-pda/measurement-principles-of-pda/. [Accessed 10 December 2021].

[21] A. L. J. S. a. S. V. Payri R., “Phase doppler measurements: System set-up optimization for characterization of a diesel nozzle,” in *Journal of Mechanical Science and Technology*, 2008, pp. 1620-1632.

[22] Solvay, *Sulphur Hexafluoride Solvay Special Chemicals,* Brussels: Solvay, 2019.

[23] P. Anne Marie Helmenstine, “ThroughtCo,” Dotdash, 1 February 2020. [Online]. Available: https://www.thoughtco.com/density-of-air-at-stp-607546. [Accessed 28 December 2021].

[24] I. R. K. W. T. Le Anh, “23 - Utilization of biofuels in diesel engines,” in *Handbook of Biofuels Production (Second Edition) Processes and Technologies*, Sawston, UK, Woodhead Publishing, 2016, pp. 699-733.

[25] M. Latarche, “Chapter Eleven - Fuel injection,” in *Pounder's Marine Diesel Engines and Gas Turbines (Tenth Edition)*, Oxford, Butterworth-Heinemann, 2021, pp. 319-357.

[26] Photron, “FASTCAM SA-X2 Datasheet,” Photron, 19 December 2017. [Online]. Available: https://photron.com/wp-content/uploads/2019/12/SA-X2_19.12.17_compressed.pdf. [Accessed 1 January 2022].

[27] Dantec Dynamics, “FlowExplorer,” 25 March 2021. [Online]. Available: https://www.dantecdynamics.com/solutions-applications/solutions/fluid-mechanics/laser-doppler-anemometry-lda/flowexplorer/. [Accessed 5 January 2022].

[28] A. C. William Emery, “Chapter 2 - Basic Electromagnetic Concepts and Applications to Optical Sensors,” in *Introduction to Satellite Remote Sensing*, Amsterdam, Elsevier, 2017, pp. 43-83.

[29] J. S. G. Valderrama, Macroscopic and microscopic characterization of non-reacting diesel sprays at low and very high injection pressures, Valencia: Universitat Politecnica de Valencia, 2018.

[30] N. N. Argilés, "PUESTA A PUNTO DE UN SISTEMA DE MEDIDA PDA", Valencia: Universitat Politechica de Valencia, 2015.

[31] V. S. R. P. J. S. L. Araneo, “Setting up a PDPA system for measurements in a Diesel spray,” *Journal of Physics: Conference Series,* vol. 45, no. 1, pp. 85-93, 2006.

[32] D. J. R. &. T. J. O. D. L. Ceman, “Calibration of the Phase Doppler Particle Analyzer,” *Aerosol Science and Technology,* vol. 18, no. 4, pp. 346-358, 1993.

[33] F. V. R. C. a. J. L. Reza Alidoost Dafsari, “Effect of aviation fuel temperature on refractive index in droplet size measurement using phase Doppler anemometry,” *Measurement Science and Technology,* vol. 30, no. 7, p. 075203, 31 May 2019.

[34] The Editors of Encyclopaedia Britannica, *Snell's law,* Chicago: Encyclopedia Britannica, 1998.

[35] Specac Limited, “The basics of polarization | Animated Guides,” 18 April 2018. [Online]. Available: https://www.specac.com/en/news/calendar/2018/04/polarization-basics. [Accessed 3 January 2022].

[36] W. V.-T. José M. García-Olivier, *DICOM V6.3 USER MANUAL,* Valencia: CMT - Motores Térmicos, 2015.